

Phased Array Antenna Element for Automotive Radar Application

by

Mohammad Hossein Nemati

Submitted to the Graduate School of Engineering and Natural Sciences

in partial fulfillment of

the requirements for the degree of

Master of Science

Sabanci University

Summer, 2014

Phased Array Antenna Element for Automotive Radar Application

APPROVED BY

Prof. Dr. İbrahim Tekin

.....

(Thesis Supervisor)

Assoc. Prof. Dr. Ayhan Bozkurt

.....

Assoc. Prof. Dr. Melih Papila

.....

DATE OF APPROVAL:

© Mohammad Hossein Nemati 2014

All Rights Reserved

Acknowledgements

I would like to offer special thanks to my supervisor Prof. Ibrahim Tekin for his help and consideration through the completion of my master study. I also like to thanks my colleagues at Sabanci University.

Phased Array Antenna Element for Automotive Radar Application

Keywords: Phased Array Radar, Patch Antenna, Surface Wave, W-band Dielectric Measurement, SiGe BiCMOS,

Abstract

In this thesis work, a design of reliable antenna front-end for W band automotive radar is studied and the problems and considerations associated with phased array antenna design at W-band are addressed. Proposed phased array antenna consists of on chip patch antenna which has the advantages of being integrated by the active circuitry. A sample of patch antenna and patch array are designed and fabricated to be tested for their functionality. Printing antenna on Silicon substrate is a compact and cost-effective approach. However, antenna on Silicon will have poor gain and will also suffer from surface wave (SW) excitation. The reason for this is Silicon high dielectric constant and loss. Surface wave can be easily excited on high dielectric constant substrate which results in gain drop and distortion in radiation pattern. To avoid substrate loss, available back etching in foundry process is used to remove the silicon under the radiating antenna and improve the gain. To kill the surface wave, a type of engineered material- called Electromagnetic Band-Gap (EBG)- is designed to filter the SW around the antenna's frequency of operation. To test the fabricated antenna, a measurement setup is implemented to do reflection coefficient and radiation pattern measurement. Measured S parameters show that there is frequency shift in response of measured antenna with respect to the simulated one. This shift can be attributed to uncertainty about the dielectric constant of Silicon at W-band. To find the exact value of Silicon dielectric constant, a measurement setup based on free space method is devised to determine the exact value of the silicon dielectric constant at W-Band frequency range.

Otomotiv Radar Uygulamaları için Faz Dizinli Anten Elemanı

Anahtar Kelimeler: Faz Dizinli Radar, Yama Anten, Yüzey Dalgası, W-bant Dielektrik Ölçümü, SiGe BiCMOS

Özet

Bu tezde, W-bant otomotiv radar için güvenilir bir ön-uç anten tasarımı anlatılmış ve W-bant'ta faz dizinli anten tasarımlarındaki sorunlara ve önemli noktalara değinilmiştir. Önerilen faz dizinli anten, aktif devrelerle entegre edilebilme avantajına sahip olan kırkık üstünde yama antenden oluşmaktadır. İşlevselliği test etmek üzere, yama anten ve anten dizini örnekleri tasarlanmış ve üretilmiştir. Antenin silikon substrat üzerine basılması kompakt ve masrafsızdır. Ancak, silikon üzerindeki antenin kazancı düşük olmakla birlikte, aynı zamanda yüzey dalgalarından (SW) da etkilenmektedir. Bunun nedeni, silikonun yüksek dielektrik sabiti ve kaybıdır. Yüzey dalgaları, kazancın düşmesine ve radyasyon paterninin bozulmasına sebep olan yüksek dielektrik sabitli substratlarda kolayca oluşabilir. Bu kayıplardan kurtulmak için, ışımaya yapan antenin altındaki silikon, üretim sürecinde ters-aşındırma ile çıkarılmış ve kazanç artırılmıştır. Yüzey dalgalarından kurtulmak için ise, antenin çalışma frekansı etrafındaki SW'yi filtreleyen özel bir Elektromanyetik Bant-Açıklığı (EBG) tasarlanmıştır. Üretilen anteni test etmek için, yansıma sabiti ve radyasyon paterni ölçen bir düzenek kurulmuştur. Ölçülen S-parametreleri incelendiğinde, simülasyonlardakine kıyasla, frekans kayması gözlenmiştir. Bu sapma, W-bant'taki silikonun dielektrik sabitinin belirsizliğinden kaynaklanmaktadır. W-bant'ta silikonun dielektrik sabitinin kesin değerini bulmak için, free-space yöntemine dayanan bir ölçüm düzeneği kurulmuştur.

Contents

ABSTRACT.....	V
ÖZET	VI
LIST OF FIGURES	VIII
1. INTRODUCTION	1
2. RADAR SYSTEM REQUIREMENTS AND CHOICE OF ANTENNA	5
2.1 ANTENNA CHOICE FOR 77GHZ SHORT RANGE RADAR SYSTEM.....	9
2.2 PATCH ANTENNA'S WORKING PRINCIPLE	10
2.2.1 Feeding Method of Patch Antenna.....	14
3. PATCH ANTENNA DESIGN FOR 77GHZ RADAR SYSTEM	19
3.1 SOLUTION FOR SURFACE WAVE PROBLEM.....	26
3.1.1 Surface wave:	27
3.1.2 Application of engineered material to filter surface wave	29
3.2 ELECTROMAGNETIC BAND-GAP META-MATERIAL:	30
3.2.1 Periodic holes:	31
3.2.2 Bumpy Surfaces.....	32
3.2.3 Uni-planar Compact photonic Band-gap (UC-PBG):	33
3.3 CHARACTERIZATION OF THE 2-D UNI-EBG STRUCTURE:.....	35
3.4 EBG-PATCH ANTENNA DESIGN:	39
3.5 ANTENNA INTEGRATION WITH ACTIVE CIRCUITRY	42

4. ANTENNA FABRICATION & MEASUREMENT RESULT	44
4.1 SIMULATED AND MEASURED RESULT:	46
4.2 DIELECTRIC CONSTANT MEASUREMENT:	48
4.2.1 Theory of dielectric constant derivation.....	49
CONCLUSION AND FUTURE WORK	56
REFERENCE.....	59

List of Figures

Fig. 2.1 RF Front End of Automotive Radar System	8
Fig. 2.2 Geometry of Patch Antenna (Top & Side View)	11
Fig. 2.3 Normalized Radiation Pattern for Microstrip (Patch) Antenna (a) E plane, (b) Hplane	12
Fig. 2.4 Side View of patch antenna with E-fields Shown Underneath	13
Fig. 2.5 Patch Antenna with an Inset Feed	15
Fig. 2.6 Patch antenna with a quarter-wavelength matching section.....	16
Fig. 2.7 Coaxial Cable Feed of Patch Antenna.....	17

Fig. 2.8 Coupled (indirect) Inset Feed	17
Fig. 2.9 Aperture Coupled Feed.....	18
Fig. 3.1 Different pattern of Substrate Etching.....	20
Fig. 3.2 Patch Antennas over Etched Silicon Substrate.....	21
Fig. 3.3 Radiation pattern on E and H plane.....	21
Fig. 3.4 Return Loss and Mutual Coupling of Array of two Patches	23
Fig. 3.5 Beam Rotation at H-Plane	24
Fig. 3.6 Radiation pattern change at (a) Eplane (b) Hplane	25
Fig. 3.7 Radiation Pattern (a)Patch with Small Substrate & (b) Patch with Large Substrate	26
Fig. 3.8 (a) dielectric coated conductor (b) Electric field(solid line) and magnetic field distribution of TM ₀ mode (c) Patch antenna first propagating mode.....	28
Fig. 3.9 Microstrip Transmission line with/without EBG	32
Fig. 3.10 Mushroom EBG structure.....	33
Fig. 3.11 Tripole Metallodielectric Photonic Band-gap (MPBG) and Uni-EBG structure .	34
Fig. 3.12 Uni-planar Compact EBG Structure Which realizes a 2D Periodic Network of LC Circuits without Introducing Vias.....	34
Fig. 3.13 Uni-planar EBG Surface and HFSS Model for unit cell of Uni-Planar EBG Surface	35
Fig. 3.14 Surface Wave Dispersion Diagram for EBG Structure	36
Fig. 3.15 Surface Wave Dispersion Diagram for EBG Structure with Doubled Size	37
Fig. 3.16 Two Different Modeling Scheme of EBG to Derive S Parameter	38

Fig. 3.17 S11 & S21 for (a) Ideal Microstrip Transmission Line (b) Line Surrounded with EBG Substrate.....	39
Fig. 3.18 Dispersion Diagram for EBG with Band-gap around 77GHz.....	40
Fig. 3.19 Designed Antenna with its S11	41
Fig. 3.20 Radiation pattern for two type of antenna	42
Fig. 4.1 Schematic of Millimeter Wave Antenna Setup.....	45
Fig. 4.2 Implemented Millimeter Wave Antenna Setup.....	46
Fig. 4.3 Simulated and Measured S11 for dipole antenna from previous work	47
Fig. 4.4 Schematic of the Measurement Setup	50
Fig. 4.5 Implemented Dielectric Setup	53
Fig. 4.6 Measured Phase Difference versus Frequency	54
Fig. 4.7 Calculated dielectric constant.....	55

1. Introduction

There are increasing application areas for automotive radar devices in cars all around the world. These devices are employed in advanced cruise control systems, which can actuate a motor vehicle's accelerator and/or brakes to control its distance separation behind another vehicle. It is anticipated that the use of these systems will become commonplace in the future, especially the civilian use of millimeter wave radars in navigation, road traffic control, safety for highway driving and security [1]. There are two bands allocated for automotive radar applications: 24 and 77-GHz band. The 24-GHz band consist of, one around 24.125GHz with BW of 200MHz, another 24GHz with BW of 5GHz for short/mid-range radars. In 77 GHz band, there is a 5 GHz bandwidth (76-77-GHz for long-range adaptive cruise control and 77-81-GHz short-range radar sensors) allocated for application of short range automotive radar for the purposes of stop and go, blind side detection, crash avoidance. Radar range resolution is inversely proportional to available bandwidth (2 GHz bandwidth corresponds to a 15 cm range resolution). As the bandwidths are much larger in millimeter wave frequencies compared to lower frequencies, for a 4-5 meter size car, 15 cm range resolution seems to be enough for detection purposes [2]. Resolution can be easily handled by the

already available wide bandwidth of 2 GHz at 77 GHz. RF-front end of radar system comprises of array of antenna followed by phase shift mechanism to make beam steering possible. The choice of antenna will be dependent on the radar requirements such as max distance and cost and ease of fabrication.

At 77 GHz, the size of the antenna becomes comparable to the chip size (less than 1 mm), and this creates the opportunity for a single-chip transceiver to be integrated with the antenna or antenna arrays. There is extensive research on designing on-chip antennas for 77 GHz band including unbalanced type of antennas such as slot and microstrip patch type antennas as well as balun circuits feeding balanced antennas like dipoles [3]. Planar type antenna like Microstrip patch antennas are good candidate for this purpose due to the advantages of low profile, light weight, and low cost [4]. So, SiGe foundry process can be used to realize overall radar system circuitry and make fabrication easy and more cost effective. However, there would be challenges for printing antenna on high dielectric constant substrate like Silicon such as gain drop and performance degradation due to unwanted surface wave and Silicon loss. In order to tackle the problems caused by surface wave in patch antenna, two approaches have been pursued to have a patch antenna with optimum performance on high-dielectric constant substrate. First method uses micromachining technology, while the second makes use of the concept of electromagnetic band-gap (EBG) structures [5]. In the first approach, part of the substrate right under the radiating element is removed to establish a low effective dielectric-constant environment for the antenna. Doing so, power loss due to surface-wave excitation is reduced and efficiency of energy coupling to space waves improves. The second approach take advantages of EBG structures: the high-permittivity substrate is engineered by putting periodic structure to change the propagation characteristic of a surface wave around antenna operative frequency. Various types of periodic loading of substrate have been studied [6]. One method is to drill a periodic pattern of holes in the substrate or ground plane. Another method is to embed a periodic pattern of metallic pads inside the substrate; pads are shorted to the ground plane with vias. In the last one, a type of planar or 2-D loading (no vias are required) were proposed which is compatible with RFIC integrated circuit fabrication technology (uni-planar electromagnetic bandgap (Uni-EBG)). This thesis work will mostly be about developing

reliable antenna system for 77GHz radar system and will address the challenges ahead of designing and fabricating antenna at W-band.

There is uncertainty about the dielectric constant of substrates such as silicon at W-band frequencies. Silicon dielectric uncertainty effect becomes very important for the design and simulations of RF circuits and antennas on silicon substrates. Designing an antenna on a substrate with inaccurate value of dielectric constant will change antenna performance and shift the resonance frequency in practice which causes large discrepancies between simulated and measured results. Simple and applicable methods for measuring the permittivity of the substrate are always in great interest of the microwave circuit and antenna designers. There are various methods for measuring dielectric constant including dielectric waveguide, cavity resonator, open resonator and free space [7]. Free space method is more suitable for wideband measurement. In free space method, the dielectric constant is measured based on either the transmission method or metal backed method [8-9]. This thesis also tries to address this issue. For this, two approaches are applied to bring out the real part of silicon dielectric constant based on transmission and reflection type measurement method. Only the phase information of the transmitted signal is used to determine the real part of the permittivity.

The thesis is organized as follow:

Chapter 2 studies the automotive radar system requirement regarding antenna and phase shifting mechanism and discusses different antenna type that can meet the radar system demands.

Chapter 3 presents the design of sample patch antenna on silicon substrate together with discussion of methods that can overcome the challenges of designing antenna on Silicon substrate.

Chapter 3 is about implementation of measurement setup at W band for antenna and dielectric constant measurement. Measured and simulated results are also presented in this chapter.

Chapter 4 presents the design of multiport single element antenna which is a parallel research study with this work. Designed antenna could have potential application in MIMO system. Finally, chapter five present the conclusion and future work in line with this work.

2. RADAR SYSTEM REQUIREMENTS AND CHOICE OF ANTENNA

Radar Technologies have been in use for defense purposes since World War II. With the advance of the solid state technology (CMOS circuits up to 100 GHz, SiGe Circuits reaching to almost 1 THz), we see more civilian use of millimeter wave radar especially in safe highway driving, navigation and traffic control. In line with these developments, ETSI has developed standards for "short range" radar for automotive applications in 24 – 77 GHz bands. In 77 GHz band, there is a 2 GHz bandwidth allocated for an application of short range automotive radar for the purposes of stop and go, blind side detection, crash avoidance, braking if crash cannot be avoided and to keep safe driving distance with the traffic ahead [1].

Radar range resolution is inversely proportional to available bandwidth (2 GHz bandwidth corresponds to a 15 cm range resolution). As the bandwidths are much larger in millimeter

wave frequencies compared to lower frequencies, for a 4-5 meter size car, 15 cm range resolution seems to be enough for detection purposes [2]. Resolution can be easily handled by the already available wide bandwidth of 2 GHz at 77 GHz. One of the critical issues at 77 GHz band and beyond is the low received signal levels. This is due to both the limited power output of the solid state power amplifiers (10-15 dBm) and also the high free space loss due to small wavelengths (at 77 GHz, at 1-meter, free space loss is -70 dB). To increase the received signal level at the receiver, one can use conventional antenna technologies such as high gain phased array design, better design of single element antennas and/or higher gain low noise amplifier. Note that at these frequencies, wavelength is on the order of a few mms, and all the system including antennas can be made on a single-chip. However, the silicon substrate for such an integrated system becomes very lossy and for the case of antennas, care should be given to design of these antennas on-chip. Radar operating range could be doubled or tripled depending on the gain of the phased array system.

Antenna gain is primary important factor which determines the range of radar system and SNR requirement. The higher the gain the higher would be the detectable range and SNR. Hand calculation can be done, based on Friis formula (equation 2.1), to determine the range and SNR for specific value of gain. For a radar system with BW=1GHz at 77GHz, the SNR can be calculated for 5m range as follow. Using antenna in array can increase the gain and result in improved SNR. Table.1 shows the link SNR budget for this scenario.

$$\begin{aligned}
P_r &= P_t G \left(\frac{1}{4\pi R} \right)^2 \sigma \left(\frac{1}{4\pi R} \right)^2 \frac{\lambda^2}{4\pi} G \\
P_r &= P_t G^2 \frac{1}{(4\pi)^3} \sigma \frac{1}{R^4} \lambda^2 \\
N &= k * T * BW \\
SNR &= \frac{P_r}{N} \\
k &= 1.38 * 1e - 23 \\
T &= 300 K \\
BW &= 1GHz
\end{aligned} \tag{2.1}$$

Table 1. SNR budget calculation

Single antenna SNR	Array antenna SNR
$P_t = 20 \text{ dBm}$	$P_t = 20 \text{ dBm}$
$G = 2 \text{ dBi}$	$G = 8 \text{ dBi}$
$R = 5 \text{ m}$	$R = 5 \text{ m}$
$\sigma = 1 \text{ m}^2$	$\sigma = 1 \text{ m}^2$
$f = 77 \text{ GHz}$	$f = 77 \text{ GHz}$
$BW = 1 \text{ GHz}$	$BW = 1 \text{ GHz}$
$SNR = -1 \text{ dB}$	$SNR = 11 \text{ dB}$

Figure 1 shows the overall topology of proposed phased array system. The radar system consists of array 4x1 antenna followed by active circuitry; the number of antenna can be increased in array for more gain. Active circuitry consists of W band LNAs and phase shifter with power combiner.

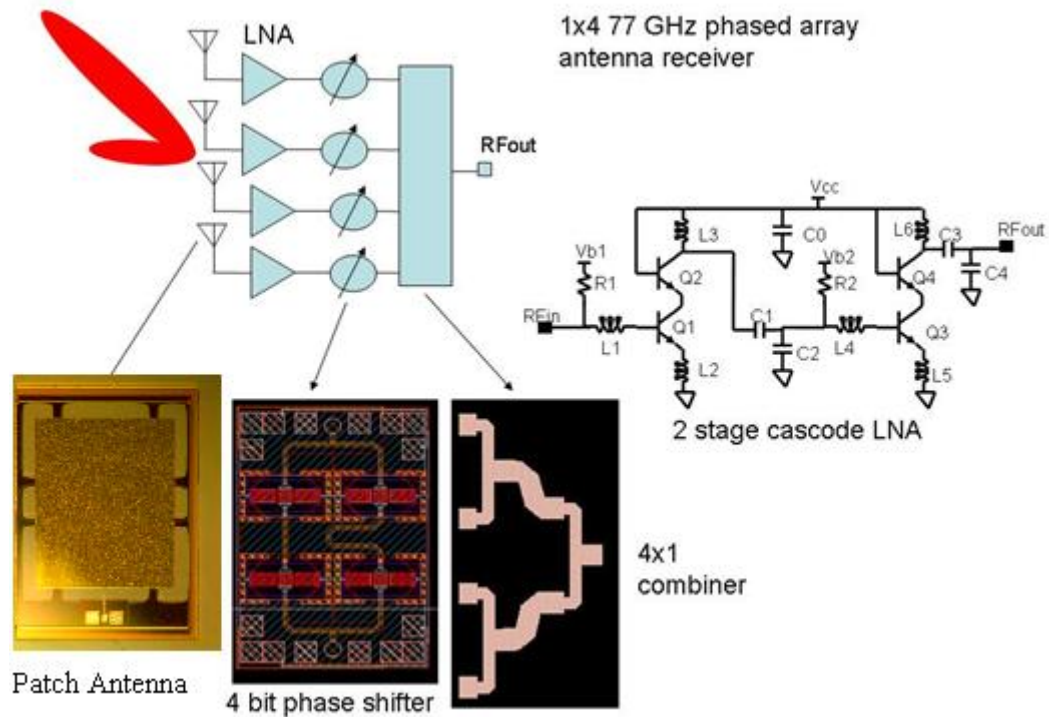


Fig. 2.1 RF Front End of Automotive Radar System

The antenna elements that will be used in the design could be a dipole, a bent-dipole and Microstrip patch antenna or even planar slot type antenna. The choice of antenna will be dependent on radar range and the assembly consideration. The output of the antenna will be amplified by a W band two stage LNA circuit. For the antenna pattern steering, a 4x1 array will be designed and each antenna line will have a very low loss MEMS based phase shifter. Using these MEMS phase shifters, the antenna main beam will be steerable. Also, one can appreciate the very low loss phase shifters, since at these frequencies; signal levels are already too low. At these frequencies, MEMS based phase shifter is preferred due to their low loss. Using IHP MEMS technology, it is already shown that low loss around 0.5 dB can be obtained. After the antenna, LNA and the phase shifter, a corporate type power combiner will be used to combine the signals coming from the four antennas. All the antennas, phase shifters, combiner and the LNA will be on the same single chip.

2.1 Antenna choice for 77GHz short range radar system

There is extensive research on designing on-chip antennas for 77GHz band including unbalanced type of antennas such as slot and microstrip patch type antennas as well as balun circuits feeding balanced antennas like dipoles [3]. The explorations and publications on various types of on-chip antennas for upper 60 GHz band show very low or negative gain without incorporating them with gain enhancement method like using reflectors. So, Conventional design of these antennas on a Silicon substrate at 77 GHz band will not generate antennas with much gain due to high silicon substrate loss and also deteriorating effect due to Surface wave. Small size of the manufactured device and the substrate effect are basic challenges and derives the interest in the methods of feeding, measuring, design and fabrication of these types of antennas. However, in our project using IHP integrated MEMS technology, substrate will be etched and since this effect is considered for the proper design of the antenna, much higher antenna gains can be obtained. Available etching technology will make it possible to remove the lossy Silicon substrate right under the radiating antenna and create low profile substrate for antenna. For surface wave undesired effects a filtering structure can be used to omit the SW around the frequency of interest. The choice of antenna will be dependent on the radar range requirement and fabrication and assembly consideration. Based on the calculation done in previous section using Friss Formula (equation 2.1), an antenna with moderate gain can fulfill the gain requirement of short range radar. Moreover, planar type antennas are attractive due to their low profile, low cost and ease of integration. Considering these two factors, the antenna elements that will be used for 77GHz short range system could be a dipole and microstrip patch antenna or even planar slot type antenna. To increase the antenna gains further in dipole case, a metal ground can be placed on one side of the dipole and bent dipole antennas to have gain around 4-5dB. For single patch antenna a gain of 8dB can be obtained. Further gain increase can be obtained by using antenna in array configuration. In this work, design of on chip patch antenna is studied. Next section will go through the basic principle of patch antenna.

2.2 Patch antenna's working principle

Microstrip patch antennas are widely used in wireless communications due to the advantages of low profile, light weight, and low cost. Recent applications have pushed the frequency into the mm-wave region for application such as automotive radars at the 77 GHz band [4]. Design of patch antenna is straight forward and there are closed form formula based on the frequency of operation and the type of substrate [10].

Figure 2.2 shows a microstrip patch antenna which is connected to main feed line by mean of microstrip transmission line. The antenna is printed on a substrate of thickness h with permittivity ϵ_r . The other side of the substrate is ground plane with dimension larger than that of patch. Both the patch and the ground plane are made of high conductivity metal and their thickness is not important. As shown in figure, the patch length is L , width W . Normally, the height of substrate h is should be a small fraction of wavelength of operation(λ), but not much smaller than 0.05λ . However, in designing patch antenna on high dielectric constant substrate like silicon care should be taken to keep the h as low as possible to couple less energy to unwanted mode inside the substrate. This unwanted inside the substrate-called surface wave- can degrade the antenna gain, radiation pattern and cross polarization.

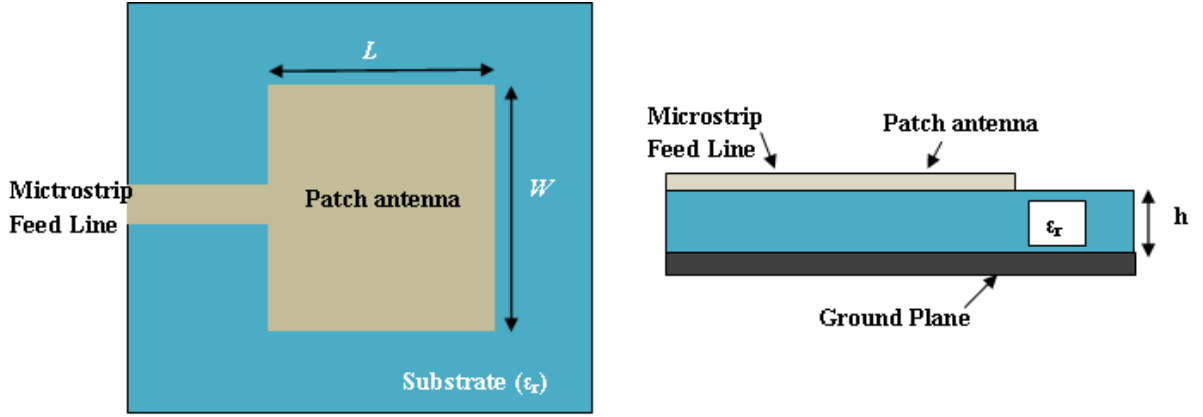


Fig. 2.2 Geometry of Patch Antenna (Top & Side View)

The length L of patch antenna determines the frequency of operation and the center frequency approximately can be expressed as:

$$f_c \approx \frac{c}{2L\sqrt{\epsilon_r}} = \frac{1}{2L\sqrt{\epsilon_0\epsilon_r\mu_0}} \quad (2.1)$$

Equation (2.1) shows that the microstrip antenna should have a length equal to one half of a guided wavelength. Guided wavelength is the wavelength inside the substrate which is smaller than that of air. The width W of the microstrip antenna determine the antenna input impedance and also the antenna bandwidth. Typically, input impedance for square patch is around 300 Ohms. Increasing the width of antenna, the impedance can be reduced and bandwidth can be increased. However, increasing the patch width will make the antenna bulky which occupy a lot of space. The width further has effect on antenna's radiation pattern. The normalized radiation pattern approximately can be expressed as:

$$E_\theta = \frac{\sin\left(\frac{KW \sin \theta \sin \phi}{2}\right)}{\frac{KW \sin \theta \sin \phi}{2}} \cos\left(\frac{kL}{2} \sin \theta \cos \phi\right) \cos \phi \quad (2.2)$$

$$E_\phi = -\frac{\sin\left(\frac{KW \sin \theta \sin \phi}{2}\right)}{\frac{KW \sin \theta \sin \phi}{2}} \cos\left(\frac{kL}{2} \sin \theta \cos \phi\right) \cos \theta \sin \phi \quad (2.3)$$

In the above, k is the free-space wave number, given by $\frac{2\pi}{\lambda}$. The magnitude of the fields, given by:

$$f(\theta, \phi) = \sqrt{E_{\theta}^2 + E_{\phi}^2} \quad (2.4)$$

Typical radiation pattern of the microstrip antenna is shown in **Figure 2.3**.

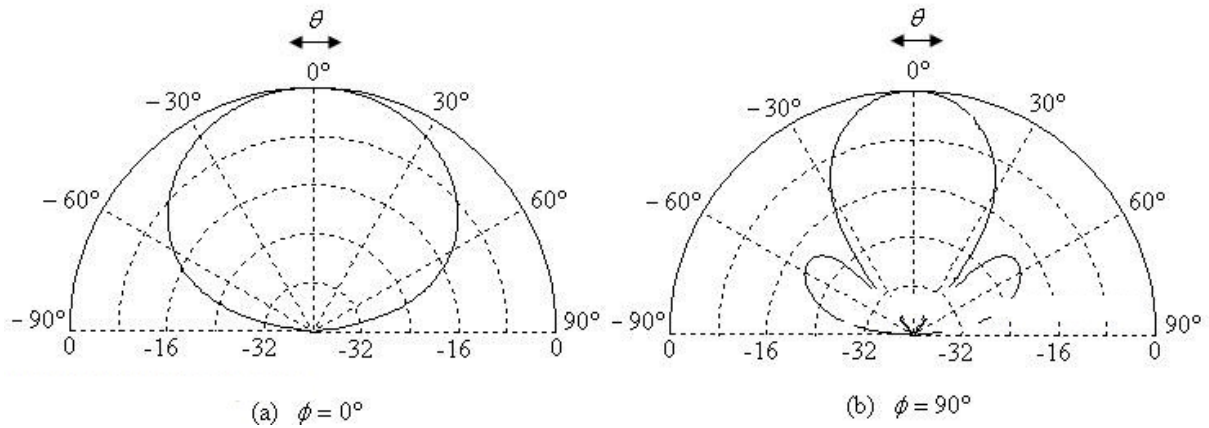


Fig. 2.3 Normalized Radiation Pattern for Microstrip (Patch) Antenna (a) E plane, (b) Hplane

In **Figure 2.3**, θ is angle from antenna broadside and the pattern is shown for E & H plane. Patch antennas have directivity around 5-7 dB. The antenna is linearly polarized and it is possible to have circular polarization by changing the feeding mechanism of the antenna. Primary drawback of patch antenna is its small bandwidth and these types of antenna are narrowband; the bandwidth of rectangular microstrip antennas is around 3%. However, the patch antenna can be modified in a way to have larger bandwidth. The reason why the patch antenna is radiating is because of fringing field around the antenna. **Figure 2.4** shows the side view of a patch antenna. Considering the current distribution on patch, it would be zero at the ends (open circuit ends) and the maximum at the center of half-wave patch. So, the current at patch input is almost zero and this low current value at the feed explains high value of impedance at patch input. Another interpretation is based on voltage distribution on patch antenna. Considering patch as open circuited transmission line, the voltage

reflection coefficient will be -1 . This means that the current and voltage distribution are out of phase with respect to each other. Therefore, the voltage is maximum (say $+V$ volts) at patch end and is minimum ($-V$ Volts). By this expression, the fields underneath the patch will look like that of **Figure 2.4**, which shows the fringing of the fields around the edges.

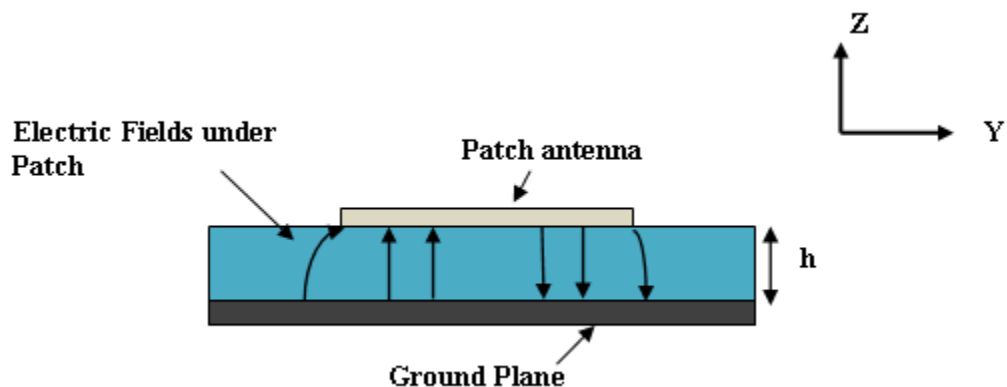


Fig. 2.4 Side View of patch antenna with E-fields Shown Underneath

Fringing fields at the patch make patch to radiate the EM wave. As shown in **Figure 2.4**, the fringing fields near the surface of the patch antenna are both in the $+y$ direction. So, the fringing E-fields on the edge of the microstrip antenna are at the same phase and add up in phase and produce the radiation of the microstrip antenna. To understand the radiation mechanism of patch it's important to know the fringing fields. The current distribution on patch cannot describe the radiation mechanism since the current distribution on patch is opposite of current distribution on ground which cancel each other. However, this can explain why microstrip transmission line does not radiate. The microstrip antenna's radiation is due to the fringing fields, which are due to the advantageous voltage distribution; hence the radiation arises due to the voltage and not the current. So, the patch antenna can be called "voltage radiator", which is different from wire antenna that radiate due to advantageous current distribution. In wire antennas, the currents add up in phase and are therefore "current radiators". An example of current radiator is dipole antenna.

It also worthwhile to mention that the smaller ϵ_r is, the fringing fields will extend farther away from the patch and make the patch better radiator. In other word, higher dielectric constant will more confine the electric field inside the substrate and decrease the radiation. Therefore, using a smaller permittivity for the substrate yields better radiation. In contrast, for microstrip transmission line, it's desired to have as less as radiation. So, a high value of ϵ_r is desirable for feed line to have less fringing filed and less radiation This is one of the trade-offs in patch antenna design. It is possible to use substrate with different permittivity for feed line section and patch antenna to improve patch radiation property and reduce that of transmission line.

2.2.1 Feeding method of patch antenna

Patch antenna can be fed in different ways: Based on the application an appropriate feeding method can be applied.

Inset Feed: as described earlier, patch antenna has high input impedance due to low current at the end ($Z = V/I$). It is possible to modify the feed and match the antenna impedance to that of 50 Ohms line. The current is low at the open ends of a half-wave patch and increases in magnitude toward the center, the input impedance ($Z = V/I$) could be reduced if the patch was fed closer to the center. One method of doing this is by using an inset feed (a distance R from the end) as shown in **Figure 2.5**.

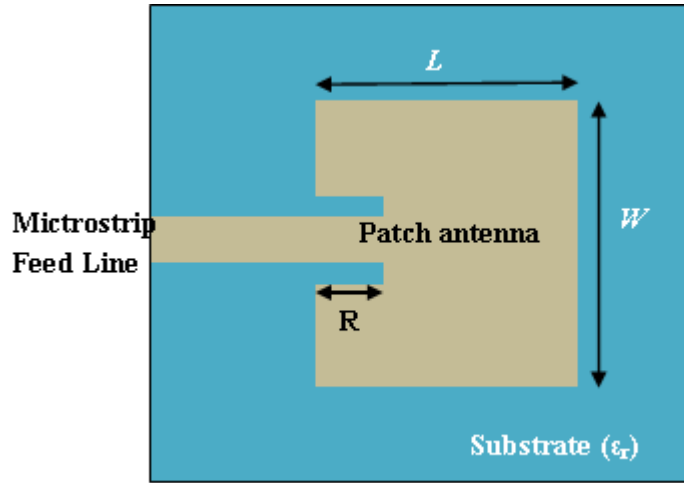


Fig. 2.5 Patch Antenna with an Inset Feed

Current has a sinusoidal distribution and moving in a distance R from the end will increase the current by $\cos\left(\frac{\pi R}{L}\right)$ - this is just noting that the wavelength is $2L$, and so the phase difference is $\frac{2\pi R}{2L} = \frac{\pi R}{L}$. The voltage also decreases in magnitude by the same amount that the current increases. Hence, using $Z = V/I$, the input impedance scales as:

$$Z_{in}(R) = \cos^2\left(\frac{\pi R}{L}\right) Z_{in}(0) \quad (2.5)$$

In the above equation, $Z_{in}(0)$ is the input impedance if the patch was fed at the end. Hence, by feeding the patch antenna as shown, the input impedance can be decreased. For example, if $R = L/4$, then $\cos\frac{\pi R}{L} = \cos\frac{\pi}{4}$, so that $[\cos(\pi/4)]^2 = 1/2$. So, a (1/8)-wavelength inset would decrease the input impedance by 50%. This method can be used to have desired value for input impedance which is 50 Ohms in normal case.

Fed with a Quarter-Wavelength Transmission Line: the microstrip antenna can also be matched to a transmission line of characteristic impedance Z_0 by using a quarter-wavelength transmission line of characteristic impedance Z_1 as shown in **Figure 2.6**.

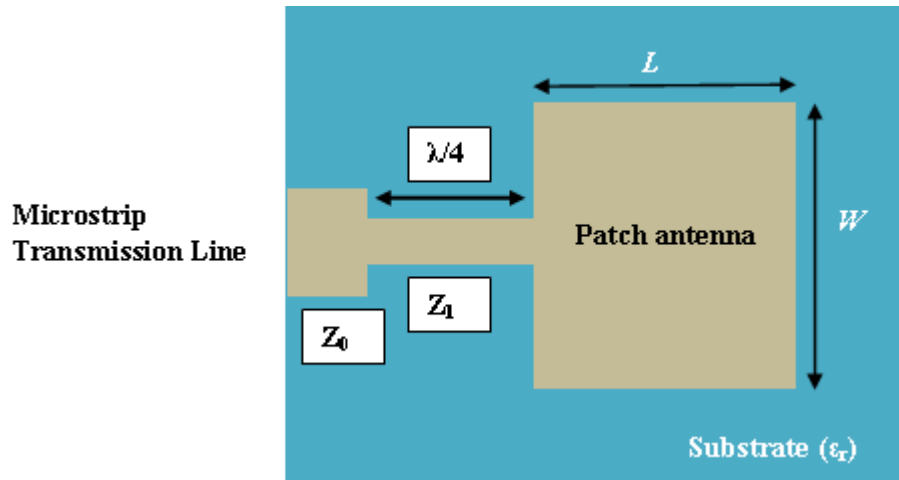


Fig. 2.6 Patch antenna with a quarter-wavelength matching section

The goal is to match the input impedance (Z_{in}) to the transmission line (Z_0). If the impedance of the antenna is Z_A , then the input impedance viewed from the beginning of the quarter-wavelength line becomes

$$Z_{in} = Z_0 = \frac{Z_1^2}{Z_A} \quad (2.6)$$

This input impedance Z_{in} , can be equated to Z_0 ($Z_{in}=Z_0$) for specific value of Z_1 and the antenna is impedance matched. The impedance Z_1 can be tuned by changing the width of the quarter-wavelength strip. To lower the characteristic impedance (Z_0) we need to make the width of strip larger.

Coaxial Cable or Probe Feed: Microstrip antennas can also be fed by coaxial cable using via that connects the patch to center conductor of patch as shown in **Figure 2.7**. The outer conductor of the coaxial cable is connected to the ground plane in other word is grounded.

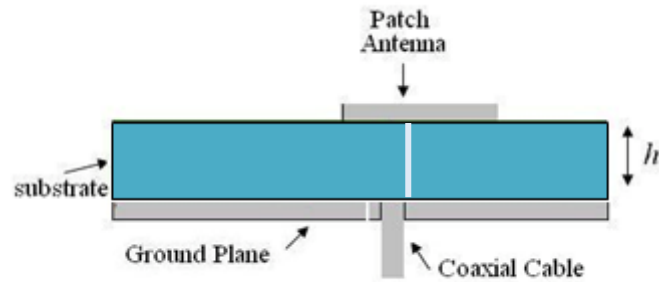


Fig. 2.7 Coaxial Cable Feed of Patch Antenna

The position of the feed can be changed to have 50 Ohm input impedance like the case of inset feed. Care should be taken about the inductance introduced by the coaxial feed. For this a height h of substrate should be considered to be low to neglect the inductance effect. In addition, the probe will also radiate, which can lead to radiation in undesirable directions.

Coupled (Indirect) Feeds: This is a non-contacting feeding method which is a modified version of inset feed. The inset feed can also be stopped just before the patch antenna, as shown in **Figure 2.8**. Moreover, the probe feed in **Figure 2.5** can be trimmed such that it does not extend all the way up to the antenna.

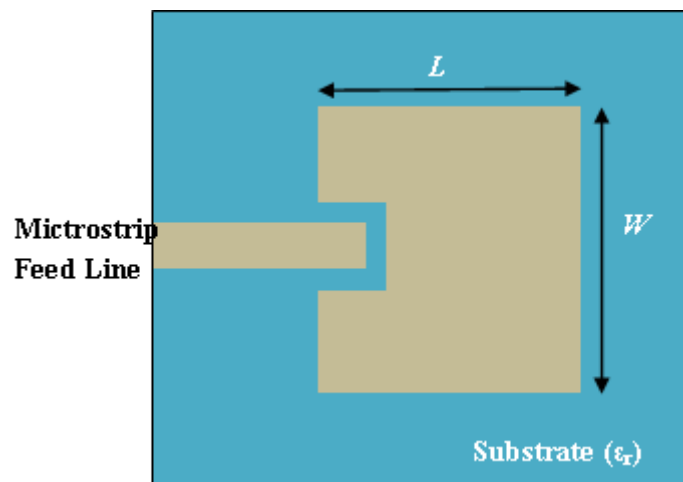


Fig. 2.8 Coupled (indirect) Inset Feed

The advantage of the coupled feed is that it adds an extra degree of freedom to the design. The gap introduces a capacitance into the feed that can cancel out the inductance added by the probe feed.

Aperture Feeds: Another method of feeding microstrip antennas is the aperture feed. In this technique, the feed circuitry (transmission line) is shielded from the antenna by a conducting plane with a hole (aperture) to transmit energy to the antenna, as shown in **Figure 2.9**.

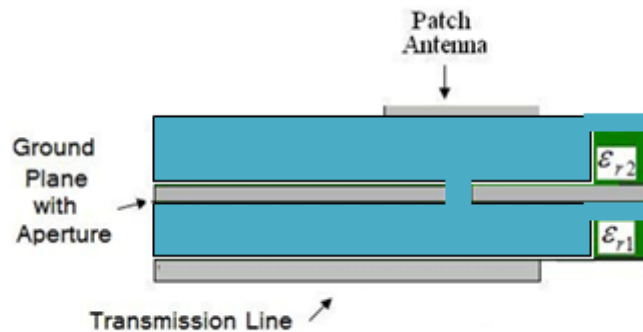


Fig. 2.9 Aperture Coupled Feed

This method is good to make patch to radiate efficiently and make the transmission line radiation less. For this purpose, the upper substrate can be made with a lower permittivity to produce more extended fringing fields, yielding better radiation. The lower substrate can be independently made with a high value of permittivity to have more confined field. The disadvantage of this method is increased difficulty in fabrication.

3. Patch Antenna Design for 77GHz Radar System

This chapter will discuss design of patch antenna at 77GHz and the challenges ahead for designing antenna on high dielectric constant substrate like Silicon. As discussed in previous chapter, design of patch antenna is straightforward and there are analytical formulas for this purpose. However, this formula can be used for patch antenna on homogeneous substrate not etched substrate; substrate etching will be used to have low profile substrate and improve antenna gain. To design antenna on etched substrate, effective dielectric constant should be calculated before using analytical formulas and it is not easy to find closed form formula for this purpose. However, it's obvious that the effective dielectric constant would be less than that of Silicon. To begin with, dielectric constant can be consider 1/8 of Silicon, then full EM simulator like HFSS can be used to numerically model the problem. Tuning the parameter, the desired resonance frequency can be obtained at 77GHz with specific value of gain.

The best way to do the etching is to remove as much as Silicon underneath the radiating element to have regarding the available etching technology. IHP SiGe technology allows rectangular shape etching with max 700x700mm and minimum of 100x100mm. **Figure 3.1** shows different etching pattern tried for antenna with maximum gain. Simulation shows that the last etching pattern is effective one regarding the gain and overall size.

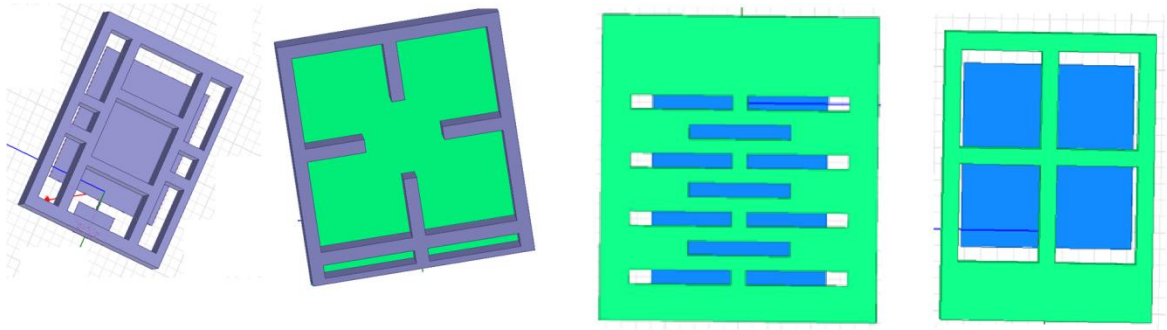


Fig. 3.1 Different pattern of Substrate Etching

Figure 3.2 shows a simple patch antenna on etched silicon substrate based on the MMIC technology available at IHP with etching pattern shown in **Figure 3.1d**. Feeding mechanism is chosen to be inset fed in order to save more area. Overall size of the antenna is 2mm^2 . Designed antenna's resonance frequency is at 77GHz and the 10dB bandwidth is about 5GHz from 75-80GHz.

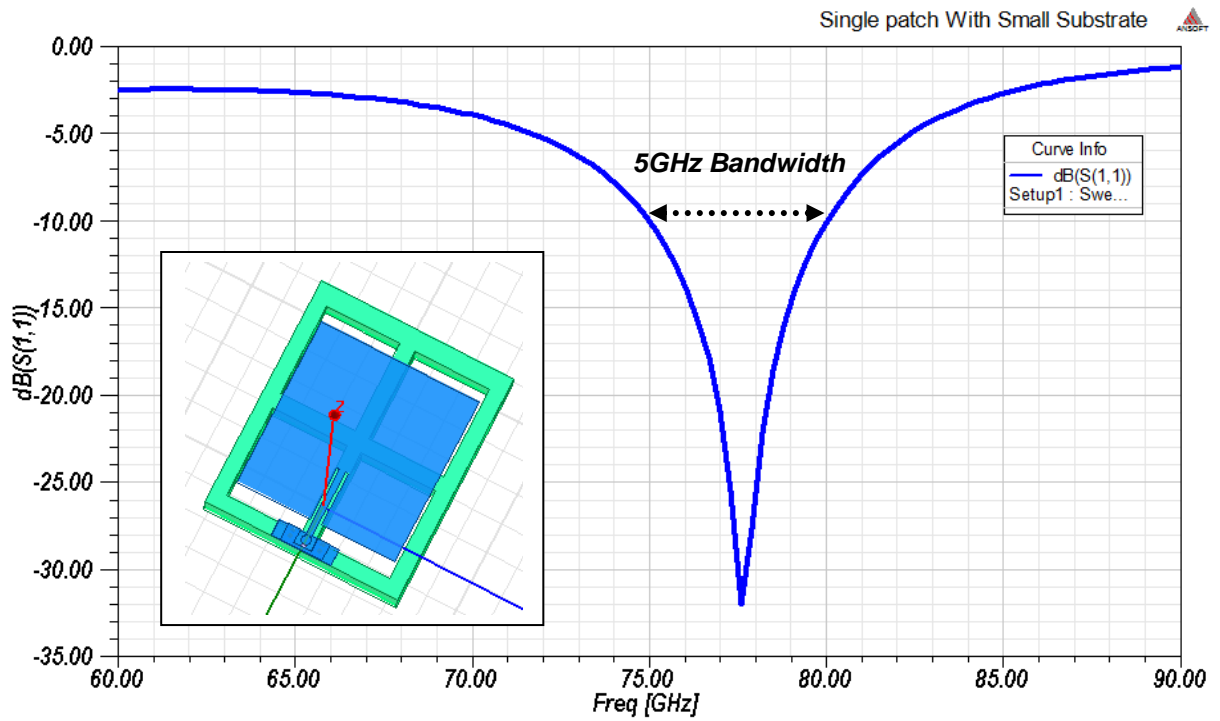


Fig. 3.2 Patch Antennas over Etched Silicon Substrate

Figure 3.3 shows the radiation pattern on E and H plane.

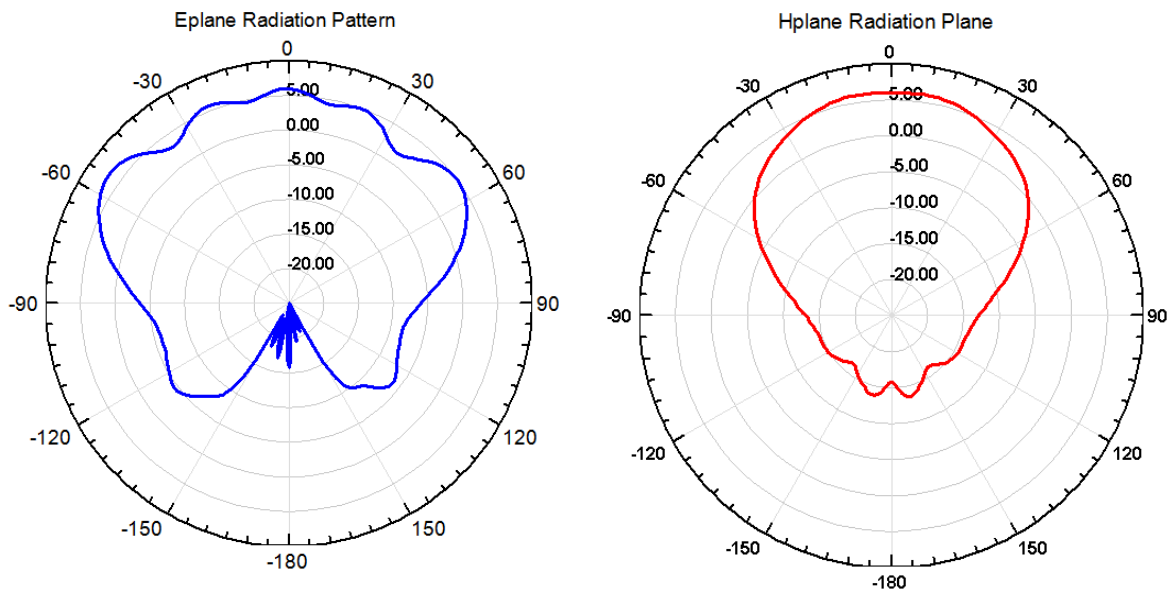


Fig. 3.3 Radiation pattern on E and H plane

Printing patch antenna on low loss and low dielectric constant substrate like FR4, the antenna will have gain of around 8dBi at broadside and undistorted radiation pattern both at E & H plane. However, using Silicon as antenna substrate will result in 2-3dB gain drop and distorted pattern especially in Eplane. This effect can be attributed to unwanted modes of propagation inside the high dielectric substrates called surface wave. The higher the dielectric constant, the higher would be the possibility of surface wave excitation. Moreover, larger height of substrate will increase the possibility of SW excitation. SW results in gain drop, pattern distortion and high cross-polarization. Moreover, the amount of energy coupled to SW increase with increase in height of substrate. So, the substrate height should be kept as low as possible. Surface wave issue will be addressed elaborately in upcoming section.

For the time being, we will focus on designing antenna system that meets requirements of phased array system. Primary requirements are high gain and beam steering capability. Designed single patch has realized gain of 5dB. To increase the radar antenna front end gain and also make the beam steering possible, array configuration can be used. To verify the concept, array of two patch antennas were designed. The beam rotation would be in patch H plane since it makes feeding network simple and also benefits from undistorted pattern at Hplane. To increase the gain more, the number of element should be increased in array. **Figure 3.4** shows return loss and mutual coupling of array with two patch elements. Mutual coupling is better than -15dB inside the band and can be further improved by increasing the spacing between the element.

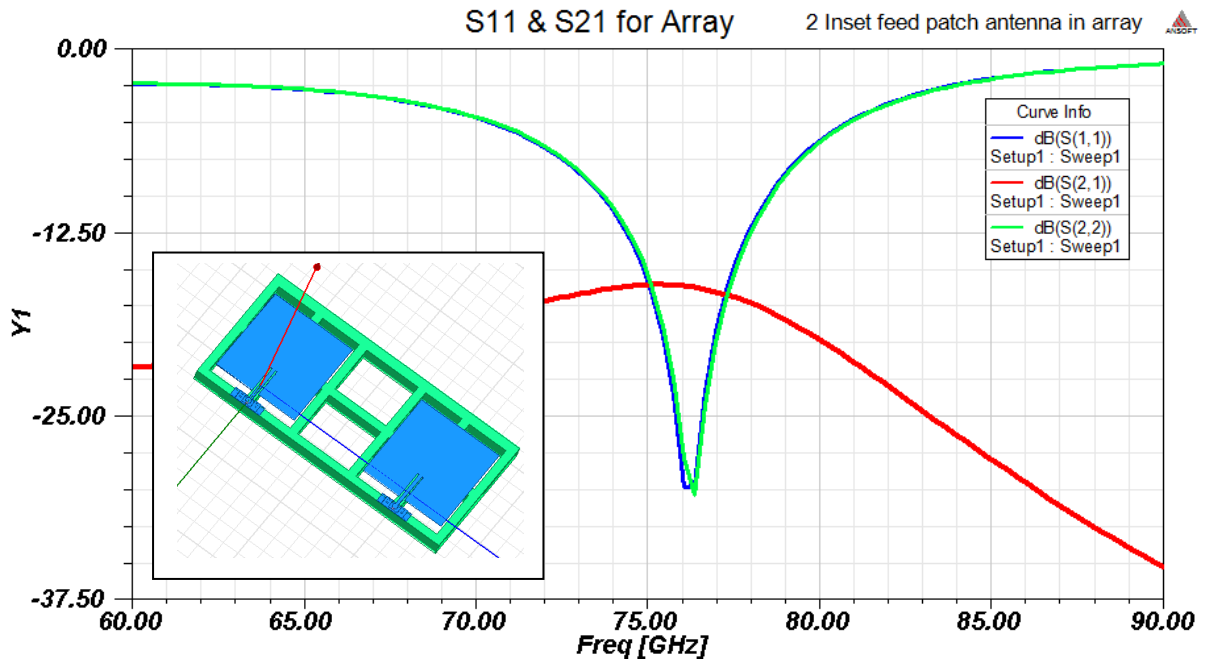


Fig. 3.4 Return Loss and Mutual Coupling of Array of two Patches

To steer the beam, phase difference should be inserted between antenna elements. In real radar system, this task will be handled by phase shifter blocks. But, for simulation purpose, HFSS has option to insert phase difference between the excitation ports. **Figure 3.5** shows the beam rotation for different values of phase shift. For phase difference of 90° between exciting ports, the beam rotates by 22° at the H-plane.

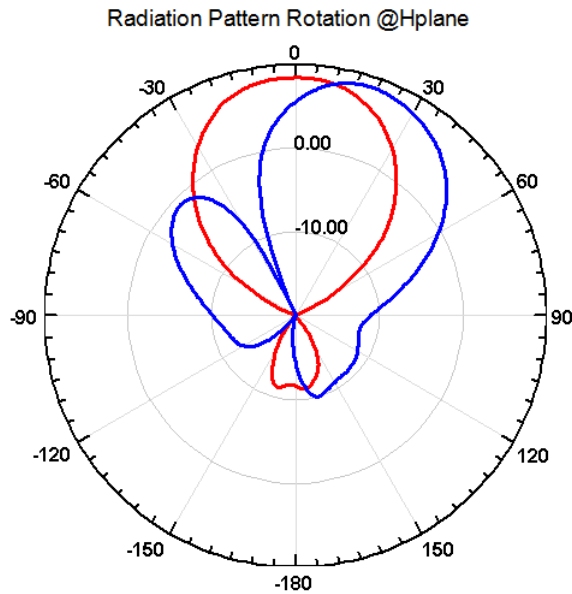
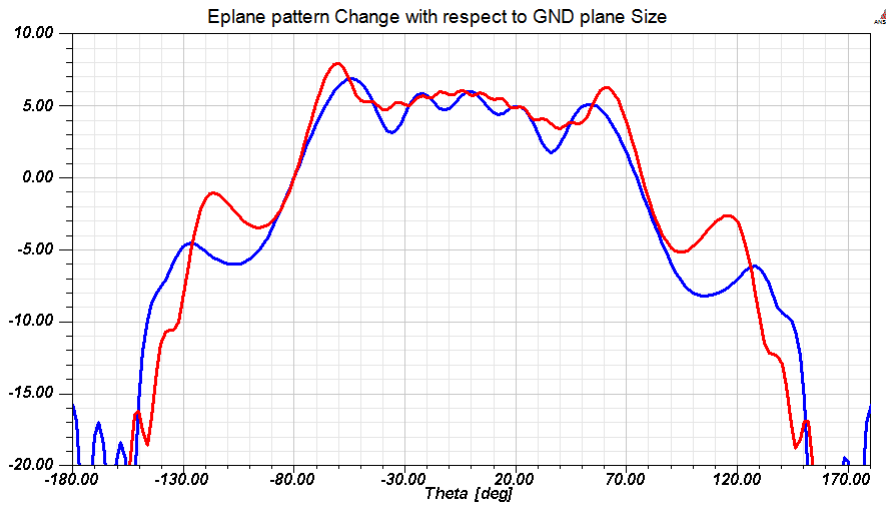
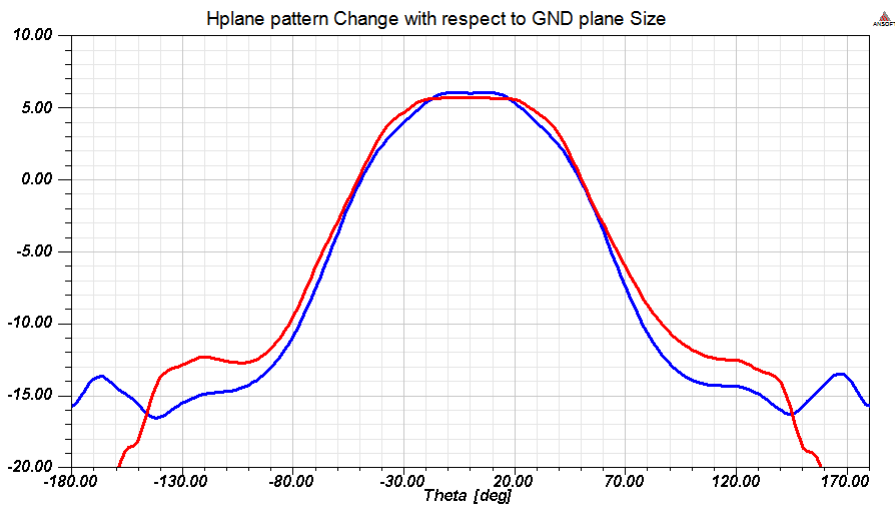


Fig. 3.5 Beam Rotation at H-Plane

As described earlier, patch antennas on high dielectric constant substrates are highly inefficient radiators due to surface wave losses. This results in a patch antenna with low gain, efficiency and distorted pattern as well as high level of cross-polarization and mutual coupling within an array environment. Surface waves are of traveling wave nature and they can be easily excited inside the silicon substrate. Patch ground plane would be low impedance medium for surface wave to propagate. So, SWs easily propagates on the ground plane and cause pattern distortion when they diffract from the edges. One consequence is that the antenna performance would be dependent on the ground plane size. Moreover, increasing the size of substrate will distort the pattern more and more. To see the deteriorating effects of SW, a sample patch antenna is simulated in HFSS for different ground plane size and also on a larger substrate. **Figure 3.6** shows the pattern change at Eplane for various ground plane size. To add up, the pattern will be the same for Hplane since SW only propagate in parallel plane to Eplane.



(a)



(b)

Fig. 3.6 Radiation pattern change at (a) Eplane (b) Hplane

Gain drops 1dB in E & H plane as the ground size enlarges by 3cm in both sides. Pattern also become more distorted in Eplnae as the ground plane size become larger. The same problem would be the case in array configuration. The problem caused by surface wave becomes more sever once the size of substrate grows larger. To see the effect of SW for

larger substrate, a comparative simulation is carried out as shown in **Figure 3.7**. As it can be seen, pattern is many more distorted for patch antenna with larger substrate.

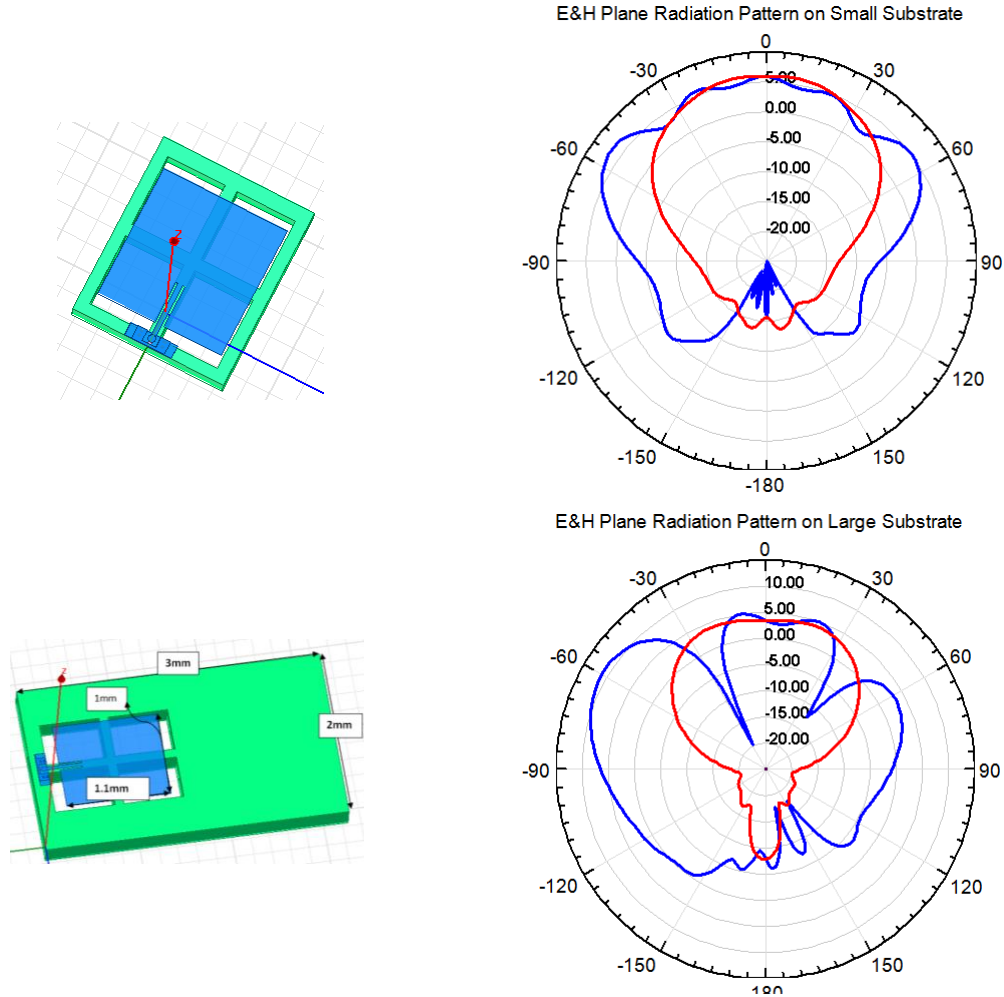


Fig. 3.7 Radiation Pattern (a)Patch with Small Substrate & (b) Patch with Large Substrate

3.1 Solution for Surface Wave Problem

Fabricating microstrip-based planar antennas on Silicon ($\epsilon_r = 11.9$) are strongly preferred for easy integration with the MMIC/RFIC and RF circuitry. However, as shown in previous section, patch antennas on high dielectric constant substrates are highly inefficient radiators due to surface wave losses and have very low gains because of localized EM waves. This

results in a patch antenna with low gain, efficiency and distorted pattern as well as high level of cross-polarization and mutual coupling within an array environment.

In order to tackle the problems caused by surface wave in patch antenna, two approaches have been pursued to have a patch antenna with optimum performance on high-dielectric constant substrate. First method uses micromachining technology, while the second makes use of the concept of electromagnetic band-gap (EBG) structures [5]. In the first approach, part of the substrate right under the radiating element is removed to establish a low effective dielectric-constant environment for the antenna. Doing so, power loss due to surface-wave excitation is reduced and efficiency of energy coupling to space waves improves. The second approach take advantages of EBG structures: the high-permittivity substrate is engineered by putting periodic structure to change the propagation characteristic of a surface wave around antenna operative frequency. Various types of periodic loading of substrate have been studied [6]. One approach is to drill a periodic pattern of holes in the substrate or ground plane. Another method is to embed a periodic pattern of metallic pads inside the substrate; pads are shorted to the ground plane with vias. In the last one, a type of planar or 2-D loading (no vias are required) were proposed which is compatible with RFIC integrated circuit fabrication technology (uni-planar electromagnetic bandgap (Uni-EBG)). Before choosing a method to mitigate surface wave problem, it will be instructive to study a surface wave nature and its characteristics.

3.1.1 Surface wave:

Surface waves can occur on the interface between two dissimilar materials, such as metal and free space or dielectric coated conductor. They are bound to the interface, and decay exponentially into the surrounding materials. At radio frequencies, the fields associated with these waves can extend thousands of wavelengths into the surrounding space, and they are often best described as surface currents. Grounded dielectric slab can support surface waves. These are propagating electromagnetic waves that are bound to the interface between slab and free space. If the interface surface is smooth and flat, the surface waves

will not couple to external plane waves. However, they will radiate vertically if scattered by bends, discontinuities, or surface texture. Surface waves appear in many situations involving antennas. On a finite ground plane, surface waves propagate until they reach an edge or corner, where they can radiate into free space. The result is a kind of multipath interference which can be seen as ripples in the radiation pattern. Moreover, if multiple antennas share the same ground plane, surface currents can cause unwanted mutual coupling [11].

Dielectric coated conductor can support both TM and TE modes [12]. The dominant mode is TM₀ with cutt of frequency of zeros. In other word, it exists in all frequencies. **Figure 3.8** shows the dielectric coated conductor together with electric, magnetic field distribution of dominant mode (TM₀) and first mode of patch antenna. As it can seen, the TM₀ modes has the same polarization as that of patch first mode. This shows that TM₀ mode can interfere with first mode of patch if it becomes excited.

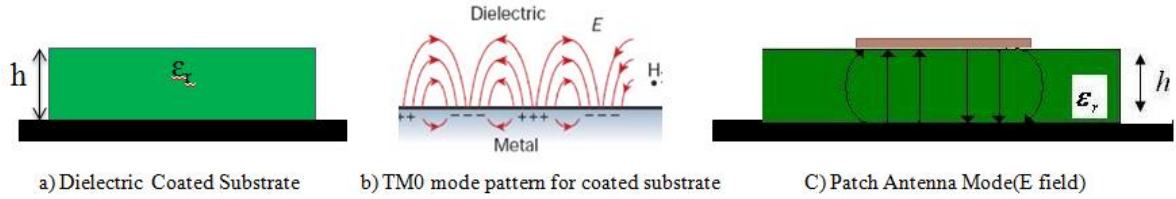


Fig. 3.8 (a) dielectric coated conductor (b) Electric field(solid line) and magnetic field distribution of TM₀ mode (c) Patch antenna first propagating mode

The cutt of frequency of modes in coated conductor is as below:

$$f_c = \frac{n}{4h\sqrt{\epsilon_d\mu_d - \epsilon_0\mu_0}} \quad \text{for TM mode: } n = 0,2,4,.. \quad (3.1)$$

$$\text{for TE mode: } n = 1,3,5,..$$

As described in previous section, engineered material can be used to filter surface wave and stop their propagation around frequency of interest.

3.1.2 Application of engineered material to filter surface wave

Metamaterials are engineered structures that exhibit electromagnetic properties not found in nature. Early in 1968, V. G. Veselago introduced the concept of left-handed (LH) materials, and described their distinct properties, such as a reversed Snell refraction, inversion of the Doppler effects, and backward Cherenkov radiation [13]. Metamaterials can be synthesized by embedding artificially fabricated inclusions in a specified host medium or on a host surface. Electromagnetic waves interact with the inclusions, inducing electric and magnetic moments, which in turn affect the macroscopic effective permittivity and permeability of the bulk composite “medium.” [14].

Meta-materials based structure can control the propagation of wave. This is accomplished with either a class of Meta-material known as photonic crystals (PC), or another class known as left-handed materials (LHM); Photonic crystal concept first introduced in optical region but later it enters the Microwave an MM-wave region where they are called Electromagnetic band-gap (EBG). Both are a novel class of artificially engineered structure, and both control and manipulate the propagation of electromagnetic waves (light). In addition, both EBG and LHM can be designed to have electromagnetic band-gap at desired frequency. In the EBG structure periodic inclusions inhibit wave propagation due to destructive interference from scattering from the periodic repetition. An EBG is a result of a Meta-material that functions in the regime where the period is an appreciable amount of the wavelength where constructive and destructive interference occur. The band-gap property of EBG makes them the EM analog of the electronic semi-conductor crystals [15]. Effective permittivity and effective permeability are basic engineering parameters of LHM metamaterials which is derived from their sub-wavelength structure. Either Negative permittivity or permeability can inhibit wave propagation. Indeed, the propagation constant is purely imaginary which result in evanescent mode in structure [16].

Microstrip antenna array on high dielectric constant substrate is of special interest due to its compact size. However, the utilization of high dielectric constant substrate can result in some drawbacks. One of the severest problems is the inevitable excitation of surface waves, which can incur strong mutual coupling among elements. The mutual coupling is one of the major sources of degradation in array performance [6]. Therefore, achieving a high degree of isolation between elements is an important approach for improving the array performance. Both EBG and LHM based structure [4-5], [17] can be applied to stop surface wave propagation around antenna's operative frequency. Hence, decrease the mutual coupling in the array.

To study MMs, there are two methods. The first choice might be a direct use (or modification) of a standard free-space method widely used in characterization of continuous materials. This method involves measurement of the transmission and reflection coefficients of a slab sample illuminated by a plane wave emanated from a highly directive antenna. One should use a rather large slab (with typical transversal dimensions of 10 wavelengths) in order to avoid diffraction at the edges. Contrary to the methods with plane-wave excitation, one may turn to the waveguide methods. The waveguide environment is well defined and completely closed, the diffraction is not present, and the testing space is rather small, relaxing the requirements on the sample size. Of course, this environment is obviously different than free space, and one should be very careful in any interpretation of the results, particularly in the case of an anisotropic metamaterial [14]. In this project, the second approach is used.

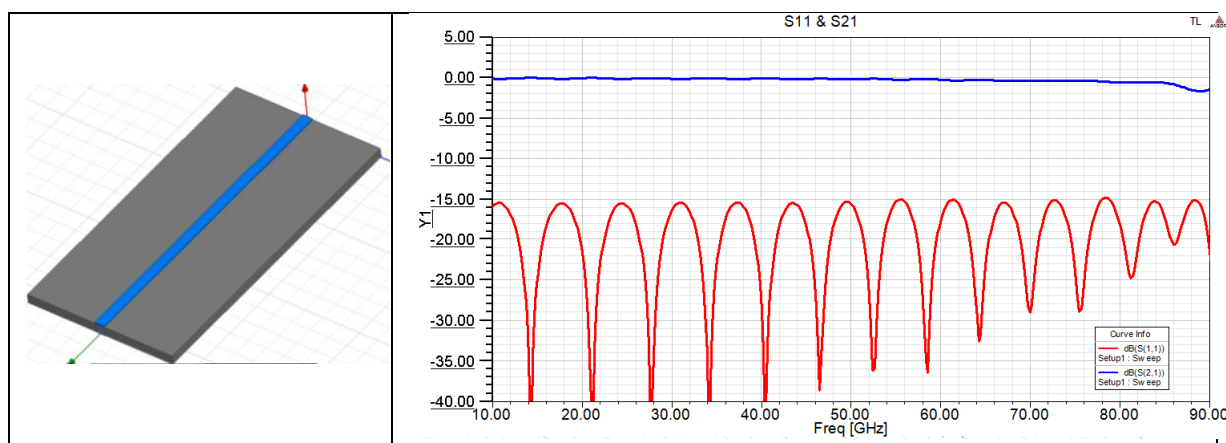
3.2 Electromagnetic Band-gap Meta-material:

As described earlier, two approaches will be followed to solve the SW problem in patch antenna. First, part of the substrate right under the radiating element is removed to establish a low effective dielectric-constant environment for the antenna. Doing so, power loss due to surface-wave excitation is reduced and efficiency of energy coupling to space waves improves. Second, EBG structure is used to filter SW: the high-permittivity substrate is

engineered by putting periodic structure to change the propagation characteristic of a surface wave around antenna operative frequency. Various types of periodic loading of substrate have been studied [6]. One approach is to drill a periodic pattern of holes in the substrate or ground plane. Another method is to embed a periodic pattern of metallic pads inside the substrate; pads are shorted to the ground plane with vias. In the last one, a type of planar or 2-D loading (no vias are required) were proposed which is compatible with RFIC integrated circuit fabrication technology (uni-planar electromagnetic bandgap (Uni-EBG)). All in all, there are three type of EBGs reported in literatures which used to control surface wave propagation. Before going through detailed design procedure for our desired EBG structure, we will look briefly over different EBG structures and study their characteristics.

3.2.1 Periodic holes:

These types of EBGs are created by drilling a periodic pattern of holes in substrate or etching a periodic pattern of circles in ground plane. To see the band-gap properties of EBG, comparative study done for simple microstrip transmission line using HFSS simulator. As shown in **Figure 3.9**, drilling periodic holes creates a forbidden frequency band for TEM mode in microstrip line. However, drilling cylindrical holes could be difficult for available foundry process. Moreover, it is possible to drill cubic holes in substrate but still fabrication cost and difficulty would be limiting factors not to use this type of EBG structure.



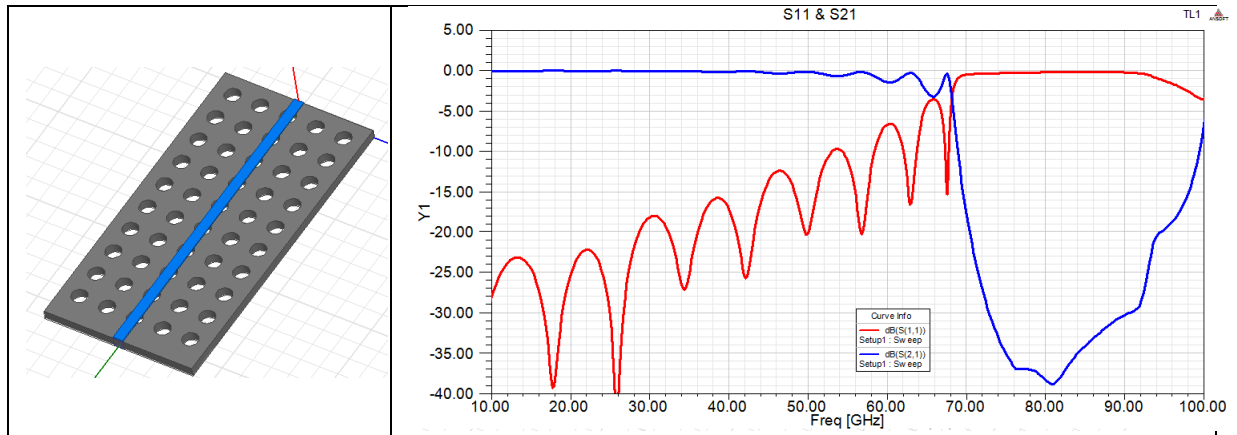


Fig. 3.9 Microstrip Transmission line with/without EBG

3.2.2 Bumpy Surfaces

Surface waves can be eliminated from a metal surface over a finite frequency band by applying a periodic texture, such as a lattice of small bumps. As surface waves scatter from the rows of bumps, the resulting interference prevents them from propagating, producing a two-dimensional electromagnetic band-gap [11].

The Sievenpiper mushroom structure is an example of such surfaces. It has been widely studied in the microwave engineering field due to its unique properties. The Sievenpiper mushroom structure basically consists of a metallic patch connected to ground with a shorting post. The general model together with HFSS model is shown in **Figure 3.10**.

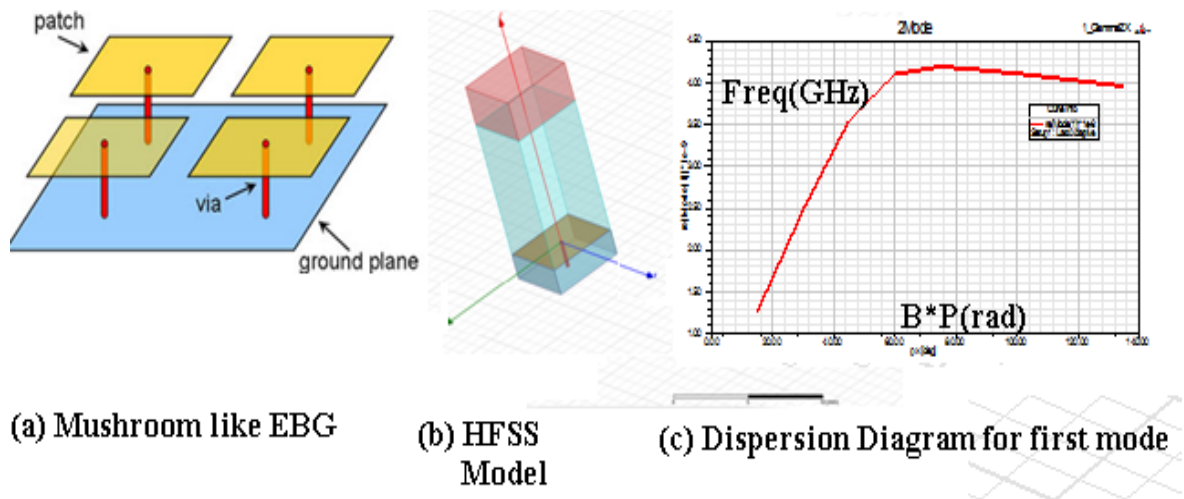


Fig. 3.10 Mushroom EBG structure

It can be used as a high-impedance surface and act like an artificial magnetic conductor. The Sievenpiper mushroom structure has also been widely used to realize left-handed Meta-materials (negative refractive index) since it can be designed to support a dominant quasi-TEM backward wave (i.e. anti-parallel group and phase velocities). It is also evident from **Figure 3.10c** that there is weak backward traveling nature associated with this structure. As depicted in **Figure 3.10c** the slop of ω - β diagram becomes negative for first dominant propagation mode. Band-gap property of this type of structure is studied with ω - β diagram. Method of analysis and the HFSS modeling of this type of EBGs will be describe in more detail in upcoming sections. To realize this EBG structure metal vias needs to be inserted inside Silicon substrate after etching is finished and this will make fabrication process complex and more expensive.

3.2.3 Uni-planar Compact photonic Ban-dgap (UC-PBG):

There is uni-planar compact photonic band-gap (UC-PBG) substrate that has some advantages over previous structures. Advantageous features of this crystal substrate include simple low-cost manufacturing (no vias are necessary) and compatibility with standard monolithic microwave integrated circuits (MMIC's) fabrication technology. **Figure 3.11** shows examples of such planar structure printed on substrate to create forbidden band.

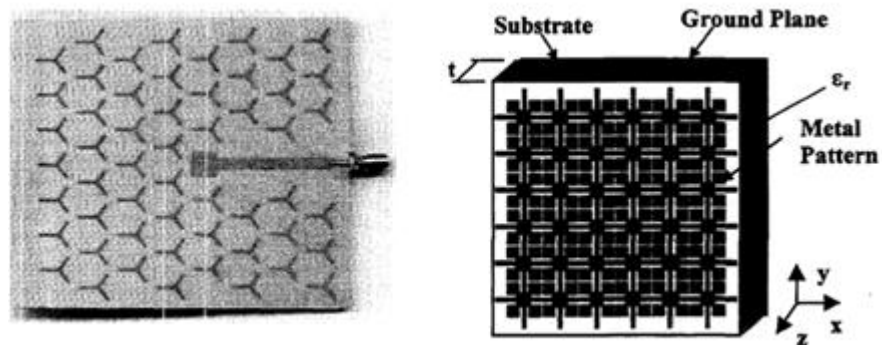


Fig. 3.11 Tripole Metallodielectric Photonic Band-gap (MPBG) and Uni-EBG structure

This work studies a square type 2-D Uni-EBG structure that is designed specifically to enhance the performance of microstrip patch antennas at 77GHz. The filtering mechanism of this structure can be explained with that of LC band-pass filter prototype as shown in **Figure 3.12**.

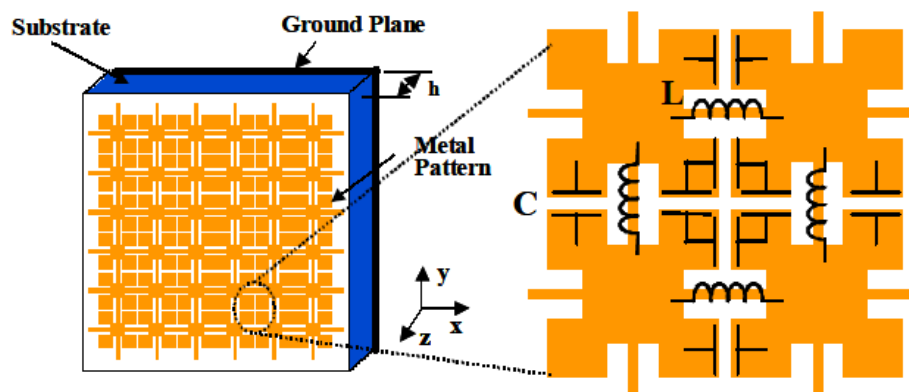


Fig. 3.12 Uni-planar Compact EBG Structure Which realizes a 2D Periodic Network of LC Circuits without Introducing Vias

First, the design procedure of 2-D surface to forbid the propagation of transverse magnetic (TM) surface waves in a grounded dielectric substrate around antenna's operative frequency elaborated. It is then demonstrated that a substantial improvement in antenna performance can be achieved simply by surrounding a microstrip patch antenna with this 2-D Uni-EBG surface, resulting in a significant increase in both antenna gain and radiation pattern.

3.3 Characterization of the 2-D Uni-EBG structure:

An EBG substrate is characterized by a dispersion or ω - β diagram. For a periodic structure such as the EBG, the field distribution of a surface wave is periodic with a proper phase delay determined by the wave number k and periodicity p . Moreover, the dispersion curve for both $k_x(\omega)$ and $k_y(\omega)$ is periodic along the k axis with a periodicity of $2\pi/p_x$ and $2\pi/p_y$: $0 \leq k_{xn} \leq 2\pi/p_x$, $0 \leq k_{yn} \leq 2\pi/p_y$, which is known as Brillouin zone [18]. **Figure 3.13** shows the geometry of our 2-D uni-planar EBG surface together with HFSS model for unit cell of EBG.

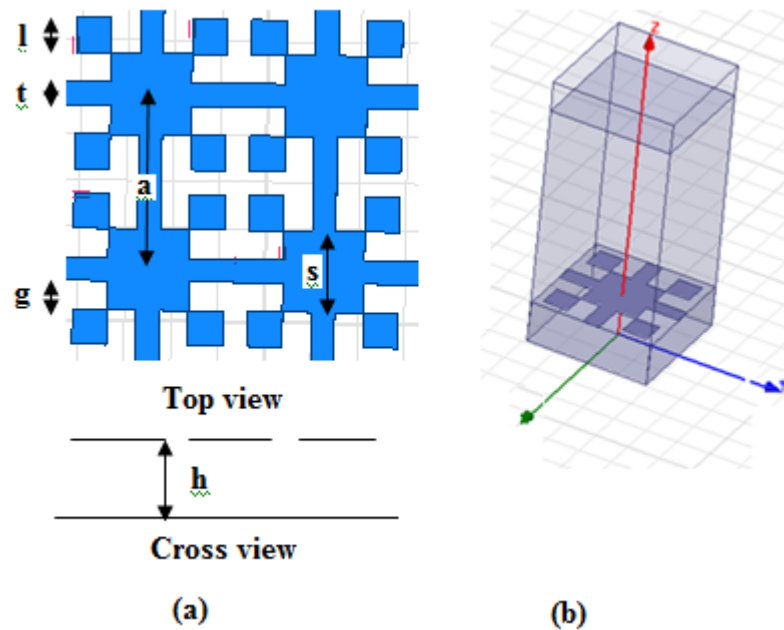


Fig. 3.13 Uni-planar EBG Surface and HFSS Model for unit cell of Uni-Planar EBG Surface

Full wave numerical method (FEM or HFSS) has been used to analyze characteristics of EBG structures with PML and periodic boundary conditions. With the utilization of periodic boundary conditions (PBCs), only a single cell of the EBG structure needs to be modeled in full wave simulation [19]. At low frequencies, the impedance is inductive and structure supports TM surface waves, while in upper bands it supports TE surface waves

due to capacitive nature of structure. In between there would be a stop-band in which no wave propagates. Surface waves with TM nature are responsible for distortion in pattern since they have same polarization with patch modes and easily harvest energy from patch mode and block the energy coupling to the space wave. So, our primary goal is to keep Surface waves with TM nature away from our frequency of interest (77GHz). On the other hand, surface wave with TE nature have orthogonal polarity with patch mode, so, for the most part, their impact can be ignored. However, their presence will degrade cross-polarization. Based on the concepts discussed above, we start to characterize the dispersion diagram of the Uni-planar EBG structure using the Ansoft HFSS. To see the typical dispersion diagram, a unit cell of this structure with $a=600\mu\text{m}$, $l=120\mu\text{m}$, $s=278\mu\text{m}$, $t=80\mu\text{m}$, $g=98\mu\text{m}$, is simulated on 250 μm thick Silicon dielectric. **Figure 3.14** shows the dispersion diagram of the surface wave's first three modes for simulated EBG structure.

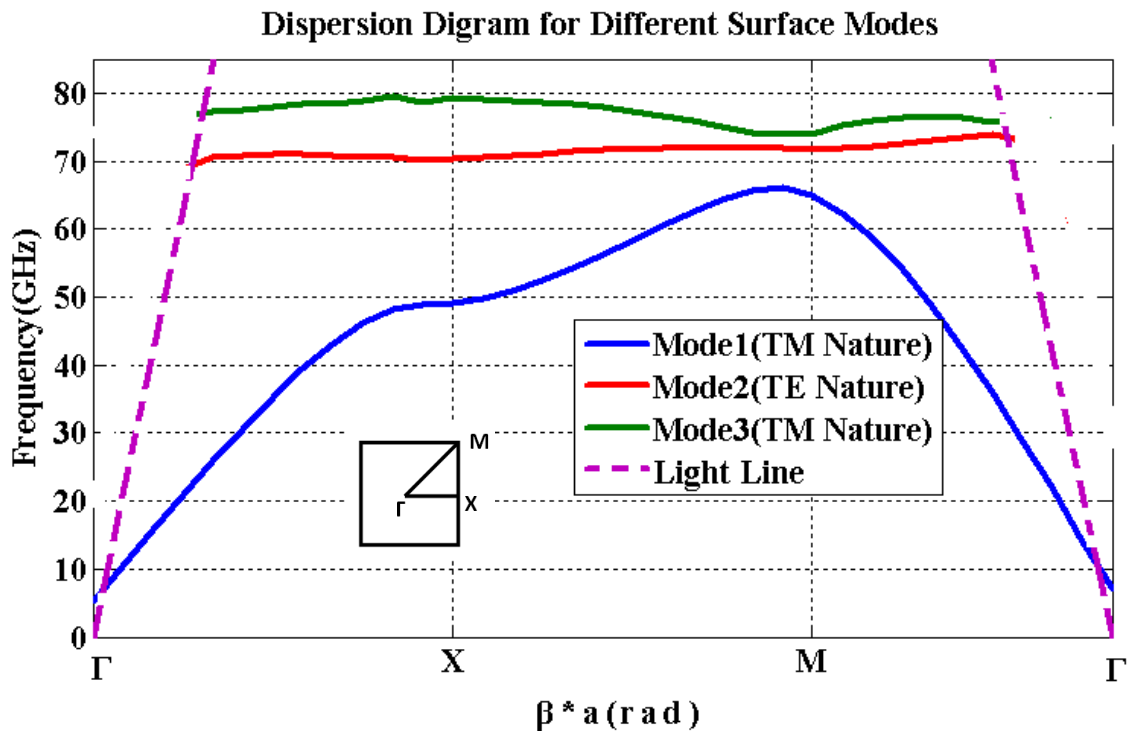


Fig. 3.14 Surface Wave Dispersion Diagram for EBG Structure

Increasing the height of the substrate will increase the probability that the surface wave can be excited. **Figure 3.15** shows the dispersion diagram once we double the height of substrate. Increasing height conceal the semi band-gap region around 70GHz, especially Γ -X propagation direction. This can be interpreted as increased probability of exciting surface wave since in thicker dielectric more energy couples to surface wave.

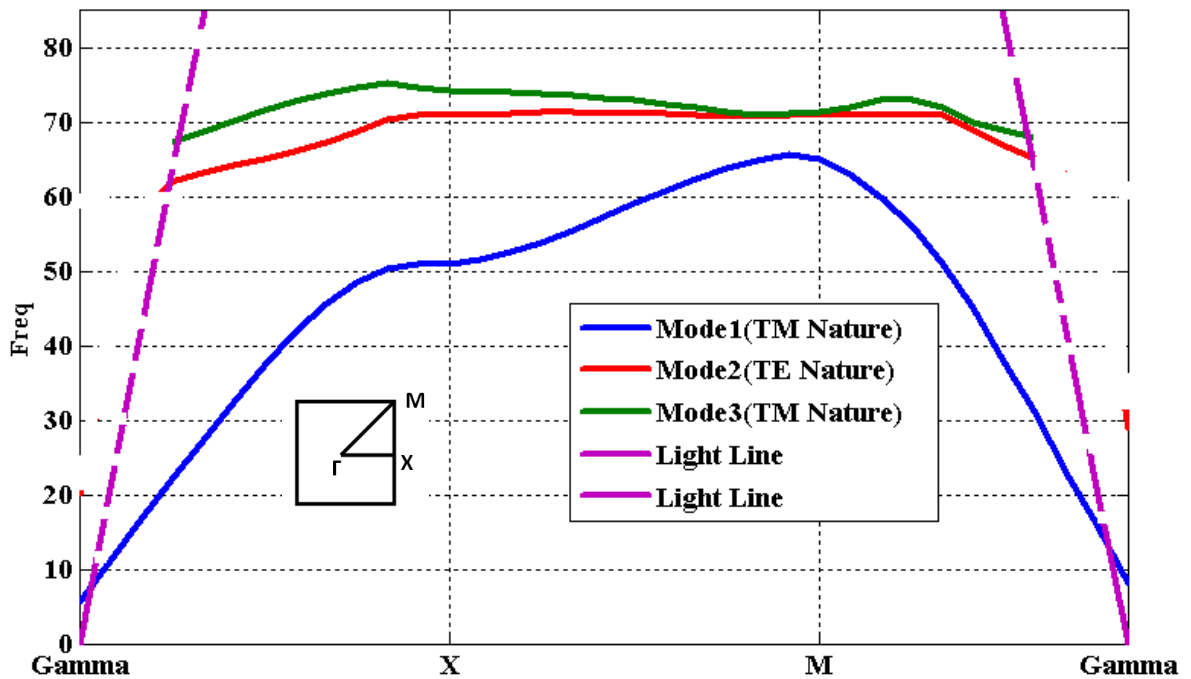


Fig. 3.15 Surface Wave Dispersion Diagram for EBG Structure with Doubled Size

An alternative method to model the EBG is by mean of S parameter. To this an ideal microstrip line can be surrounded by EBG structure and filtering properties can be studied based on obtained S parameter. Below is the two simulation scenario for characterizing the EBG structure.

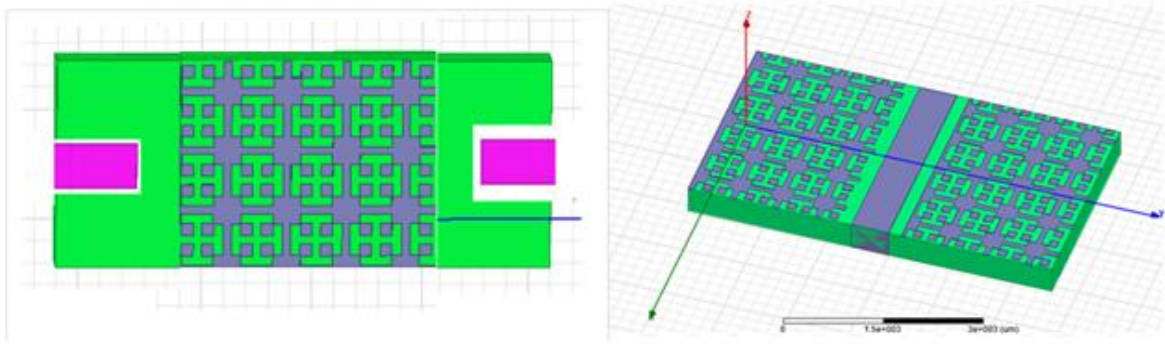
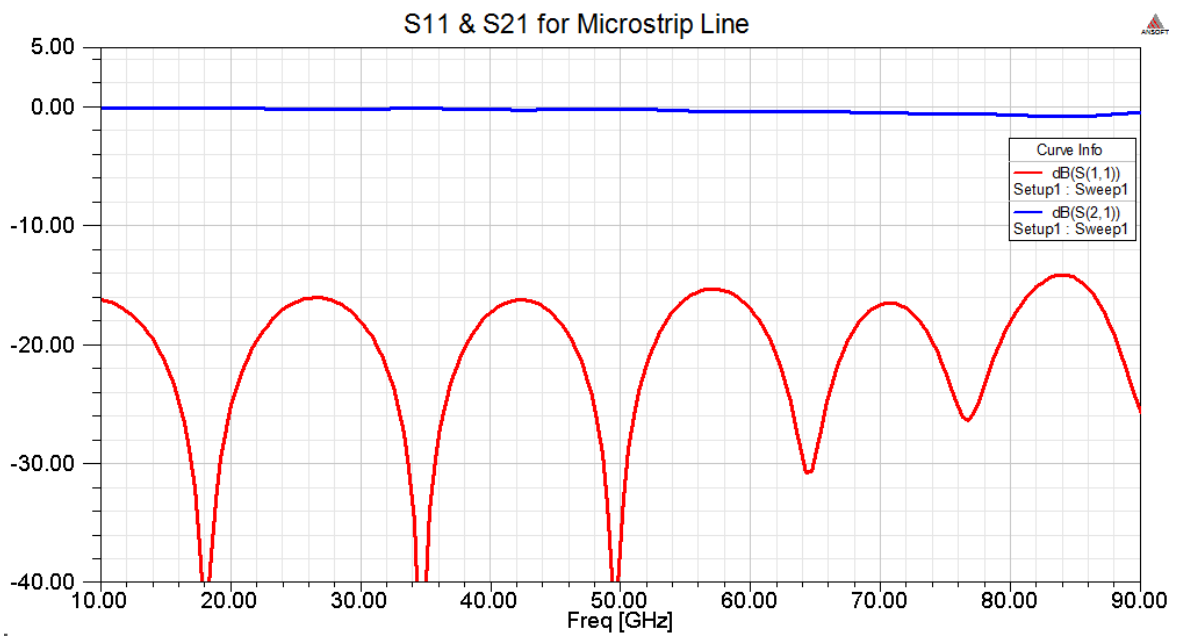
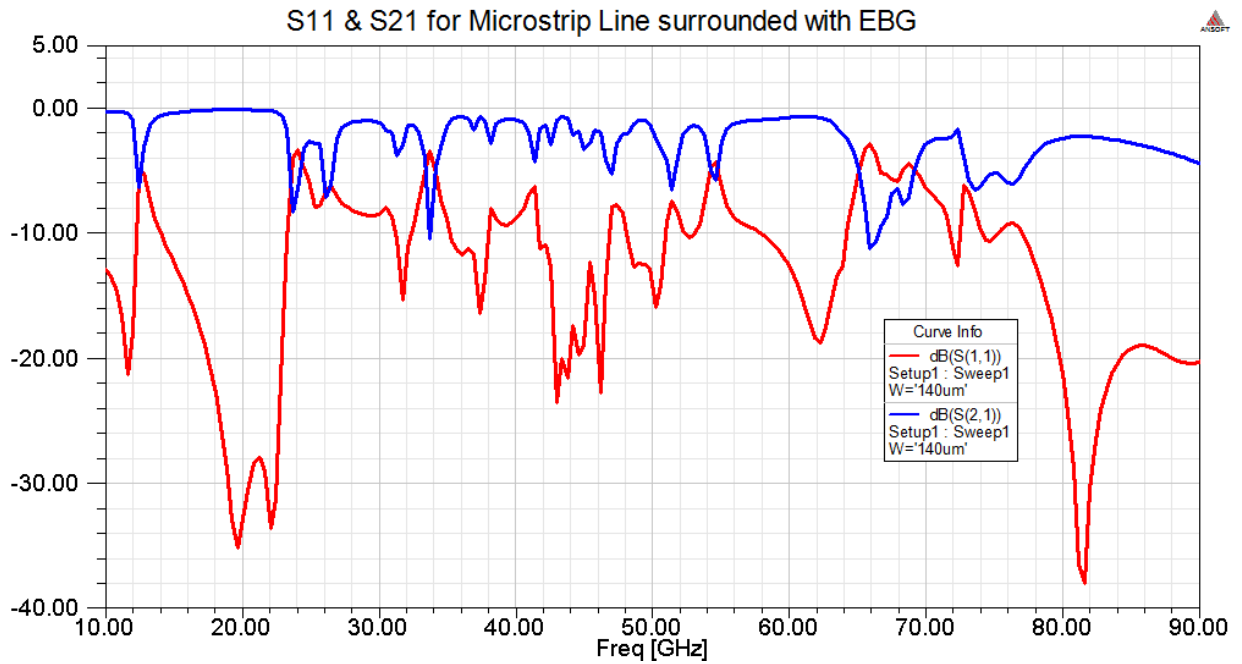


Fig. 3.16 Two Different Modeling Scheme of EBG to Derive S Parameter

Below is the result for s parameter modeling of EBG structure.



(a)



(b)

Fig. 3.17 S11 & S21 for (a) Ideal Microstrip Transmission Line (b) Line Surrounded with EBG Substrate

Figure 3.17 shows not completely but to some extent the filtering property of the EBG structure. From this simulation result it can be decided that the dispersion or ω - β diagram characterization yield better result.

3.4 EBG-Patch Antenna design:

Once the proper EBG surface has been designed for surface wave suppression, the design of an EBG antenna is straightforward. This is done simply by surrounding the antenna with EBG surface (**Figure 3.19**). The EBG surface does not interfere with the near field of the antenna, and it just suppresses the surface waves [15]. However, the presence of the EBG near the patch drops the resonance frequency which can be removed easily by tuning the length of the patch. As discussed earlier based on pattern distortion, in patch antenna, surface wave mostly are present at Eplane. So, it enough for designed EBG only to have band-gap in this Eplane and filter surface wave with propagation direction in Eplane. Γ -X

direction of Brillouin zone is correspondence of patch Eplane and characterizes the surface wave that exists inside the patch substrate. So, to save computational resources, proposed EBG will be characterizing in Γ -X plane. Simulation in HFSS is performed as described earlier for an EBG with band-gap around 77GHz. **Figure 3.18** shows the dispersion diagram of finalized structure with band-gap around our frequency of operation (77GHz). The simulation is done considering first five modes. Starting from mode one which is of TM nature then the nature of mode change to TE and continue switching between TM and TE. The nature of first mode can be attributed to the inductive property of the structure at low frequency. Remembering the LC band-pass filter model described earlier, one can discern why this structure is inductive at low frequency. Moreover, the mode propagation diagram is trimmed by light line since for the propagation constant smaller than that of line light the mode will be evanescent. Desired band-region is shown in **Figure 3.18** that is between 72-77GHz.

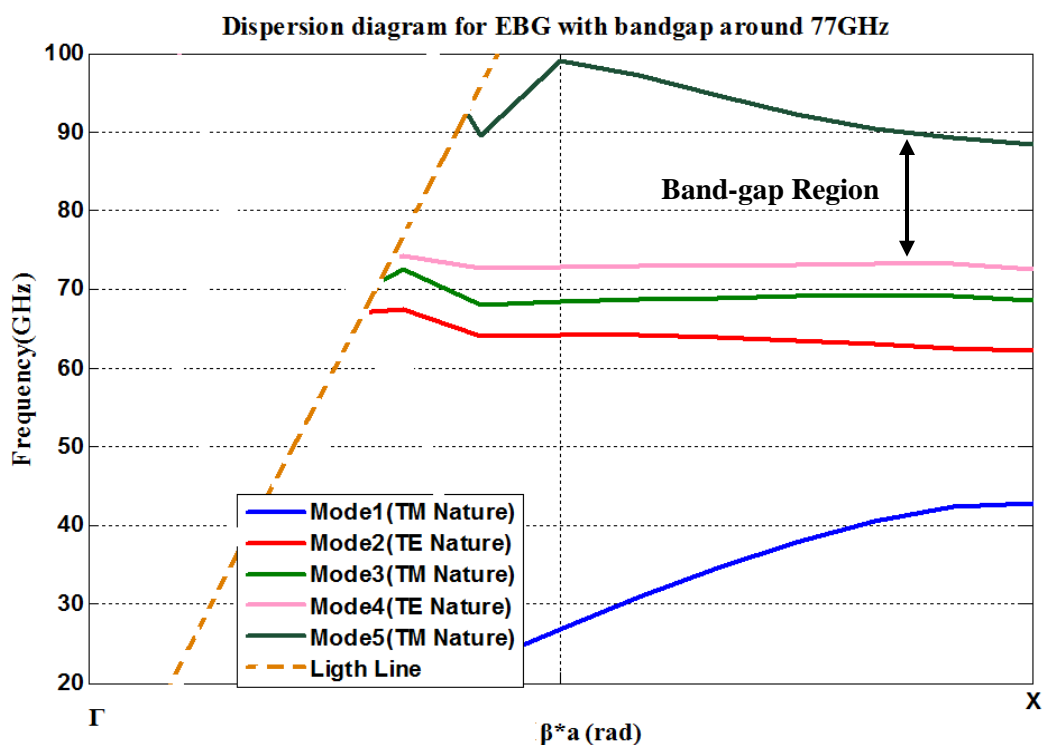


Fig. 3.18 Dispersion Diagram for EBG with Band-gap around 77GHz

The next step is to surround the patch antenna with proposed EBG Substrate and check for its performance. **Figure 3.19** shows patch antenna with EBG around together with antenna's S11.

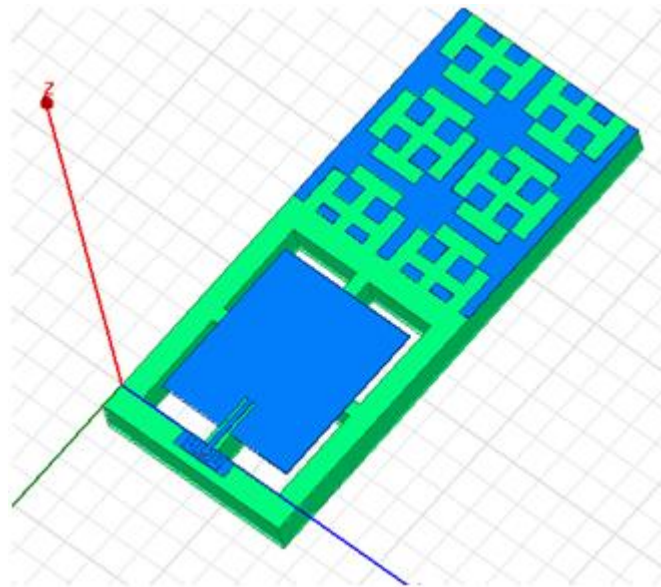
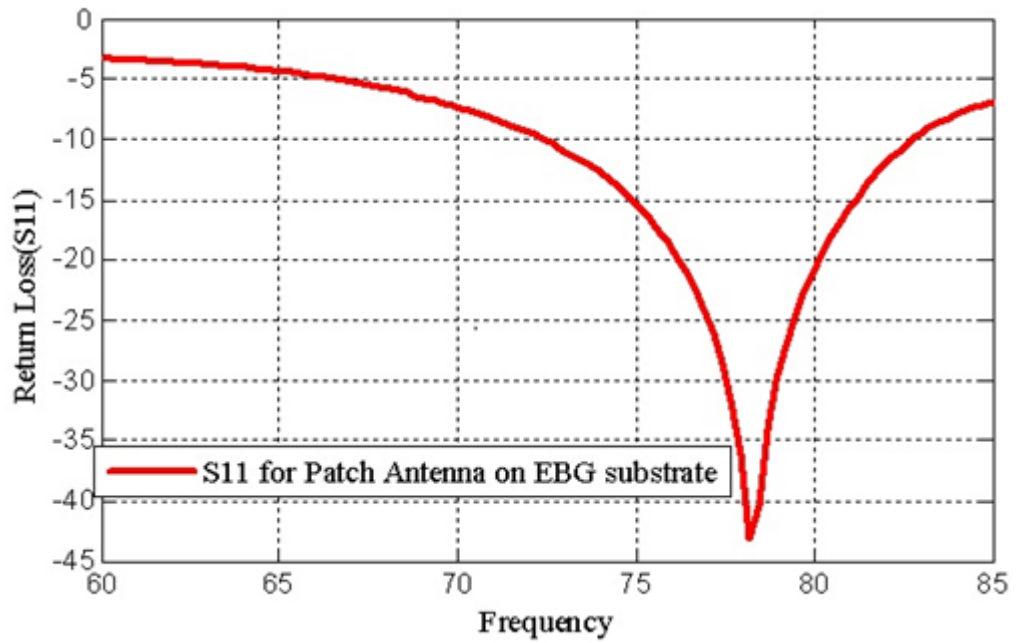


Fig. 3.19 Designed Antenna with its S11

For comparison purposes, another patch antenna designed on a same substrate without EBG surface. **Figure 3.20** compares the radiation pattern and gain of these antennas, both in the E and Hplane.

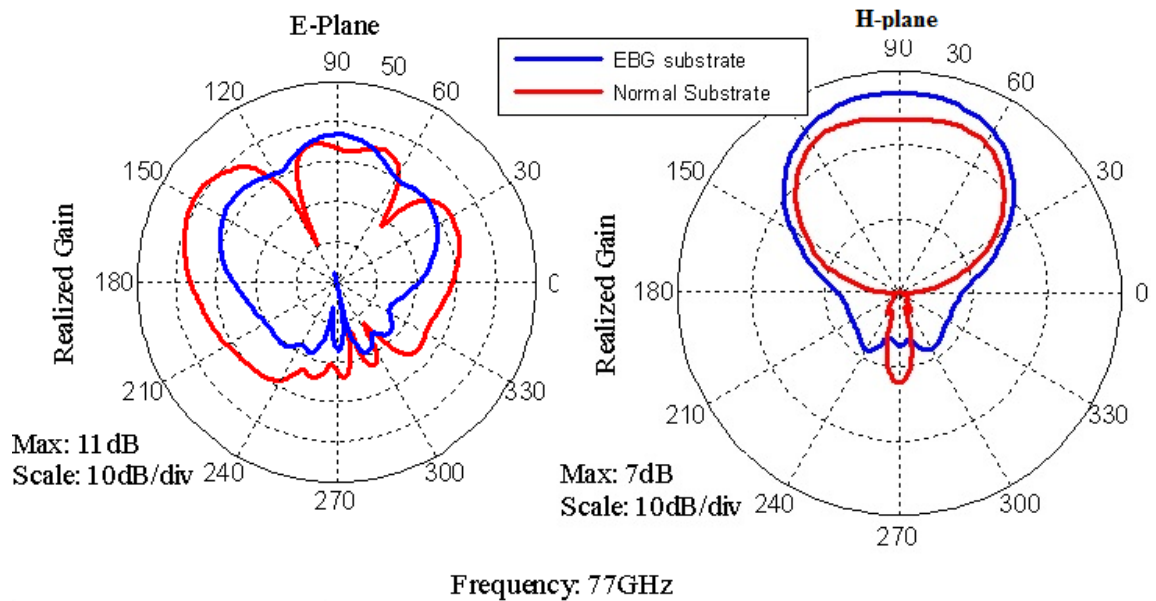


Fig. 3.20 Radiation pattern for two type of antenna

Designed antennas are submitted for fabrication and next chapter will provide the measurement result.

3.5 Antenna integration with active circuitry

As described earlier, radar system RF front end consist of array of antenna with LNAs and phase shifter. The output of the antenna will be amplified by LNA circuit. For the antenna pattern steering, a 2x1 array is designed and each antenna line has a very low loss MEMS based phase shifter. Using these MEMS phase shifters, the antenna main beam will be steerable. Also, one can appreciate the very low loss phase shifters, since at these frequencies; signal levels are already too low. At these frequencies, MEMS based phase shifter is preferred due to their low loss. Using IHP MEMS technology, it is already shown that low loss around 0.5 dB can be obtained. After the antenna, LNA and the phase shifter,

a corporate type power combiner will be used to combine the signals coming from the two antennas. All the antennas, phase shifters, combiner and the LNA will be on the same single chip.

An array of two patch antennas integrated with LNA and phase shifter is submitted to be fabricated by IHP.

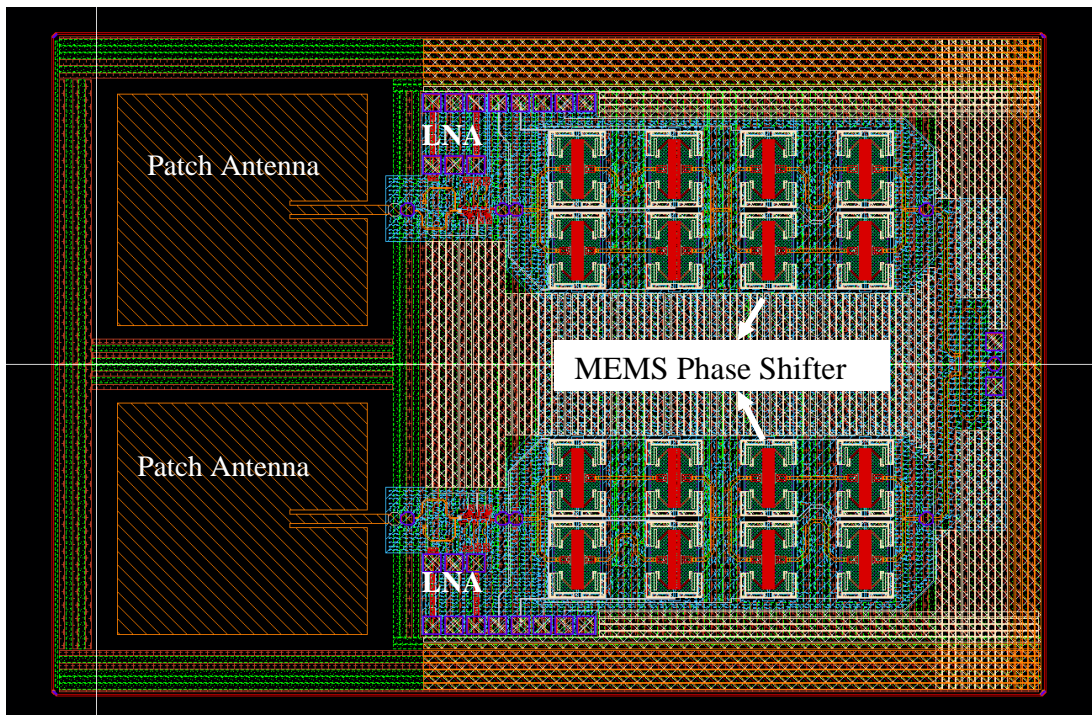


Fig. 3.21 Layout of Phased Array RF Front-End

4. Antenna Fabrication & Measurement Result

Millimeter wave technology brings about many promising feature such as possibility of high speed communication, less interference, etc. However, conducting practical experiments at this frequency band could be challenging and will require high-tech devices and skilled experimenters. First challenge is the high losses which make it necessary to consider transmitted power level, proper signal amplification and component spacing. For antenna measurement, anechoic chamber can be used up for frequency up to 50GHz. However, for 75-110GHz, a setup similar to that of anechoic chamber needs to be implemented outside the chamber. Outdoor setup occupies less space and also makes it possible to better connect the antenna to measuring probes. Our antenna measurement setup at Sabanci University seeks to fulfill these necessities and make reliable measurement possible. To do so, our measurement setup follows all the standard procedure in antenna measurement. **Figure 4.1** shows schematic of outdoor antenna setup block that consists of Network analyzer, standard horn antenna, extender, GSG probe and rotatable arms.

Moreover, waveguide to coaxial adaptor is used in different part for transition purpose. Measurement follow the same rule applied in anechoic chamber.

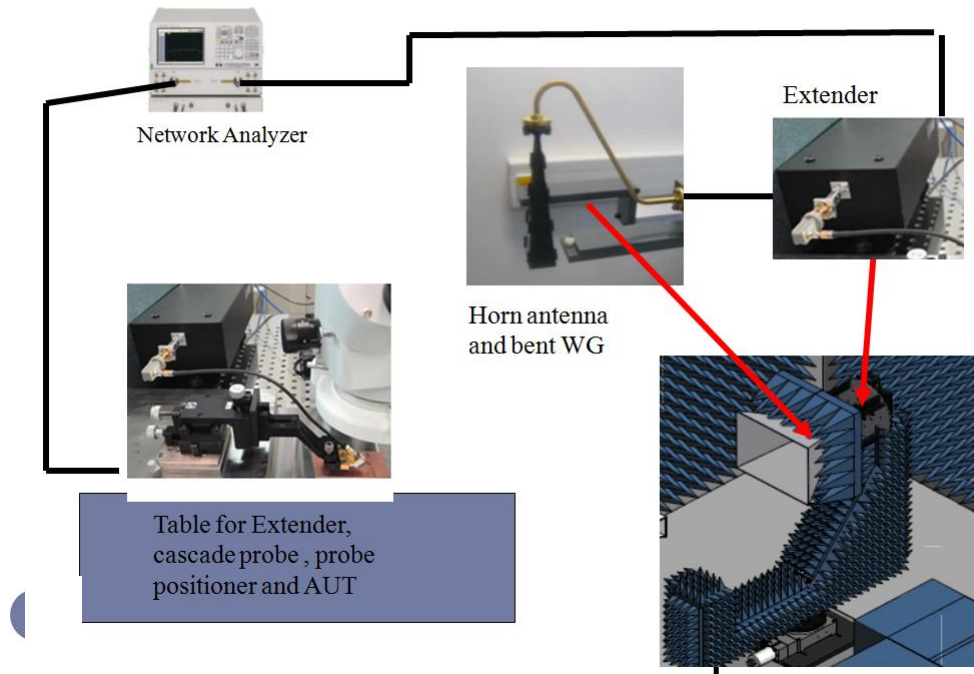


Fig. 4.1 Schematic of Millimeter Wave Antenna Setup

GSG probe is used to connect the antenna under test (AUT) to signal source. There are knobs places on GSG probe for fine adjustment in different direction. GSG probe is connected to Network analyzer (NA), with extender block in between. Extender serves the purpose of signal frequency up conversion to convert 300MHz-50GHz signal from NA to 75-110GHz necessary for W-band measurement. To measure the field radiated by AUT, a standard horn with known gain is used. This horn is installed on collecting arm capable of rotating 180° at elevation plane. Care should be taken to place horn antenna in far field region of AUT not too far to lose signal level. Another type of GSG probe is available with 90° rotations with previous one. This probe make it possible to put AUT in 90° rotated with respect to previous case and switch from antenna's E to H plane and vice versa. Besides, the standard horn can be rotated in 90° to its original position and make it possible to determine

the co- and cross-polarization at E and H plane. This setup enables reflection coefficient, gain and far-field radiation pattern measurement. Our antenna under the test (AUT) is dipole antenna and simple inset-fed patch antenna surrounded by EBG structure. A sample of the antennas has been realized by MMIC technology available at IHP, Germany. **Figure 4.2** shows an implemented setup picture at SUNUM.



Fig. 4.2 Implemented Millimeter Wave Antenna Setup

4.1 Simulated and measured result:

At the time of writing this thesis, we were waiting for our patch antenna from IHP to be shipped to us. But, to see the functionality of the implemented setup, a sample of dipole antenna and patch antenna from previous works has been measured by setup described

earlier. **Figure 4.3** shows the measured and simulated result for dipole antenna printed on etched silicon substrate. As it can be seen, there is a frequency shift in response of the measured result. This change can be attributed to uncertainty about exact value of Silicon dielectric constant. There is no reliable reference presenting exact value of silicon dielectric constant at W-band. To have correct model of substrate at simulation, dielectric constant needs to be determined. So, the next section of this thesis will be about finding value of silicon dielectric constant based of available methods.

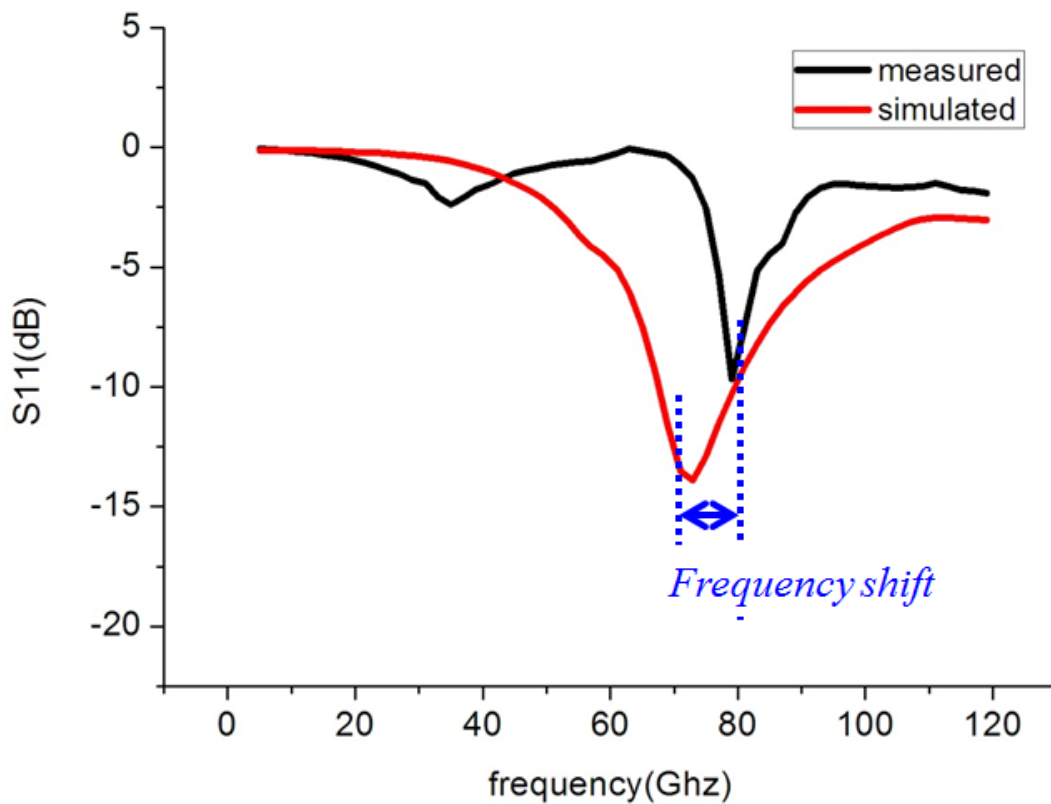
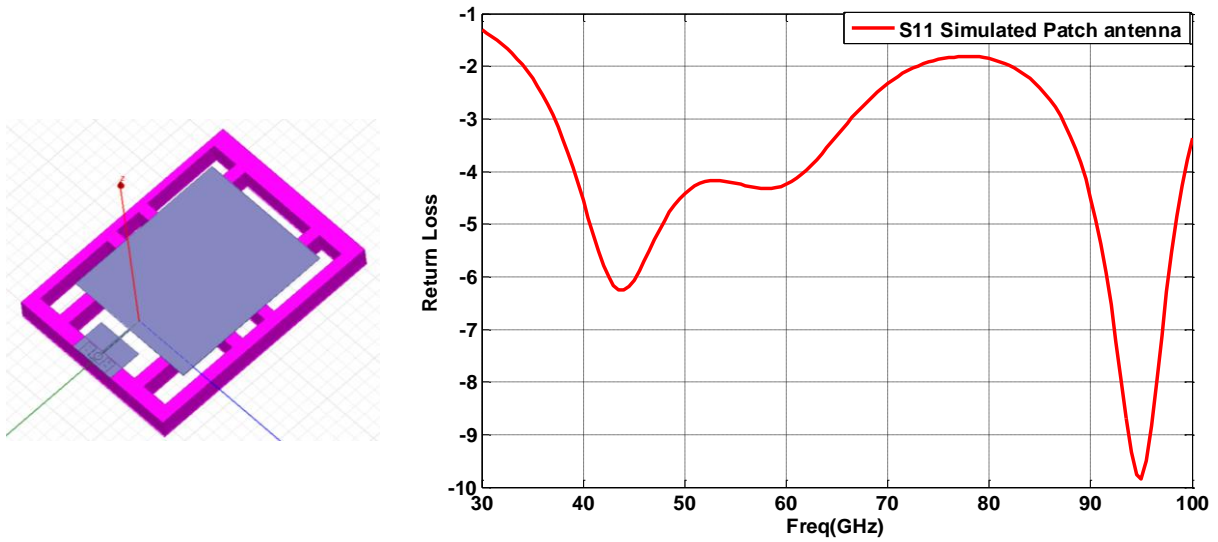
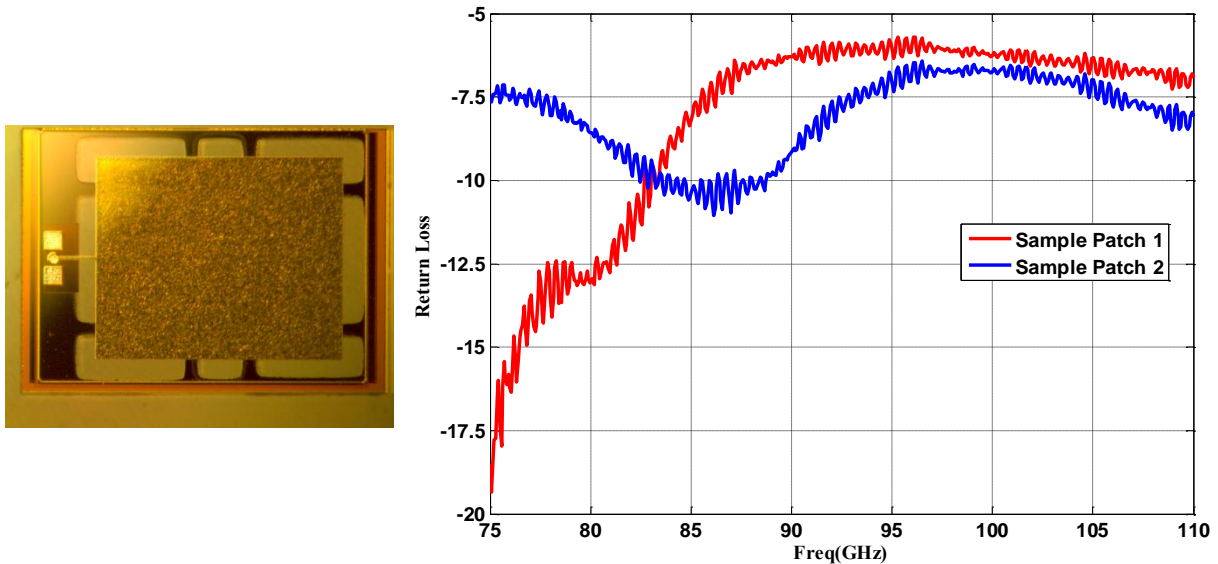


Fig. 4.3 Simulated and Measured S11 for dipole antenna

Figure 4.4 shows simulated and measured result for a sample patch antenna from previous work.



(a) Simulated patch antenna with its reflection coefficient



(b) Fabricated patch antenna with its reflection coefficient

Fig. 4.4 Measured and simulated result for sample patch antenna

4.2 Dielectric constant measurement:

There is uncertainty about the dielectric constant of substrates such as silicon at W-band frequencies. Silicon dielectric uncertainty effect becomes very important for the design and

simulations of RF circuits and antennas on silicon substrates. Designing an antenna on a substrate with inaccurate value of dielectric constant will change antenna performance and shift the resonance frequency in practice which causes large discrepancies between simulated and measured results. Simple and applicable methods for measuring the permittivity of the substrate are always in great interest of the microwave circuit and antenna designers.

There are various methods for measuring dielectric constant including dielectric waveguide, cavity resonator, open resonator and free space method which is more suitable for wideband measurement [7]. In free space method, the dielectric constant is measured based on either the transmission method or metal backed method [8-9]. Metal backed method is better for very thin dielectric samples. However, some disadvantages such as edge diffraction and multiple reflections are associated with the free space method. Edge diffraction can be minimized by using spot focus antenna which produce Gaussian beam by mean of lens and also taking the sample size large enough, while time domain filtering and LRL (line, reflect, line) calibration technique can be used for multiple reflection problem.

Using amplitude and phase information it is possible to derive both real and imaginary parts of dielectric constant. However, it is possible to derive only the real part just using the phase information of either transmitted or reflected signal. In this work, two approaches are applied to bring out the real part of silicon dielectric constant based on transmission and reflection type measurement method. Note that no calibration and time domain filtering is utilized in the measurements. The transmitter and receiver antennas which are used in the measurement set-up have wide beamwidth far away from Gaussian beam. Only the phase information of the transmitted signal is used to determine the real part of the permittivity.

4.2.1 Theory of dielectric constant derivation

Travel time of EM wave is different for different Medias and this time difference can be interpreted as phase difference in frequency domain. A slab of silicon wafer with dielectric

constant of ϵ_1 is placed in the far fields of the two horn antennas as shown in **Figure 4.4**. Thickness of the DUT is supposed to be d_1 , while d_0+d_1 is the total distance between the two antennas. Impedance variation in the direction of wave propagation will cause multi-reflections inside the silicon sheet and infinite series of rays with different phase difference will be picked up by the receiver antenna (Ant. 2 in Fig. 1). S_{21} between two antennas can be calculated for the configuration of the **Figure 4.4** which is confined to the air (ϵ_0) at both sides of the DUT.

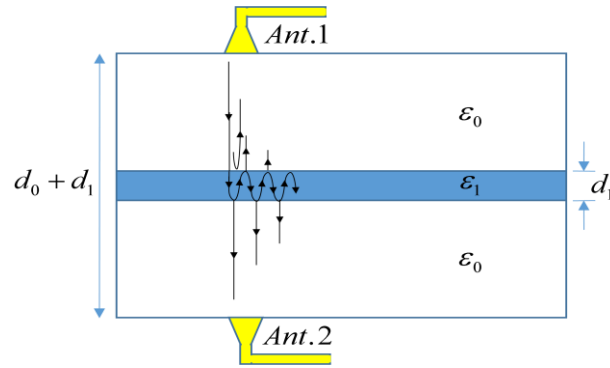


Fig. 4.5 Schematic of the Measurement Setup

Analytical relation for S_{21} is obtained as follow,

$$\begin{aligned}
 S_{21} &= e^{-jk_0 d_0} T_{21} e^{-jk_1 d_1} T_{12} + e^{-jk_0 d_0} T_{21} e^{-j3k_1 d_1} \Gamma_{12} \Gamma_{12} T_{12} + \dots \\
 &= e^{-j(k_0 d_0 + k_1 d_1)} T_{21} T_{12} (1 + \Gamma^2 e^{-j2k_1 d_1} + \Gamma^4 e^{-j4k_1 d_1} + \dots) \\
 &= e^{-j(k_0 d_0 + k_1 d_1)} T_{21} T_{12} / (1 - \Gamma^2 e^{-j2k_1 d_1}), \quad |\Gamma| < 1
 \end{aligned} \tag{4.1}$$

where T_{21} and T_{12} are transmission coefficients from air to dielectric and vice versa, respectively.

Γ_{12} is reflection coefficient from dielectric to air and is defined as:

$$\Gamma = \Gamma_{12} = \frac{\sqrt{\epsilon_r} - 1}{\sqrt{\epsilon_r} + 1} \tag{4.2}$$

and

$$k_i = \omega \sqrt{\mu_0 \epsilon_i}, \quad i = 0,1 \quad (4.3)$$

which is wave-number in each of the media.

Accurate measured phase between transceiver antennas will be

$$\begin{aligned} \varphi_{S_{21}} = & -(k_0 d_0 + k_1 d_1) \\ & - \tan^{-1}(\sin(2k_1 d_1) / (\Gamma^{-2} - \cos(2k_1 d_1))) \end{aligned} \quad (4.4)$$

which is deduced from relation (4.1). We can use phase of the measured S21 and (4.4) with determined d_0+d_1 and d_1 to calculate the permittivity of silicon at the measured frequency. In this case, accurate values of measured phase, transceiver antennas spacing and dielectric thickness is needed to achieve accuracy in the calculated ϵ_r .

In the proposed method, phase of S21 is measured in two cases; 1) Silicon sheet is placed between the antennas. 2) Silicon is absent between the antennas.

Phase difference between two cases can be calculated by subtracting relation in (4.4) when the silicon is between the antennas and silicon is replaced by air (by setting $\epsilon_r = 1$ or $\Gamma = 0$ in (4.4)).

$$\begin{aligned} \Delta \varphi = \varphi_{S_{21}} \Big|_{air} - \varphi_{S_{21}} \Big|_{sub.} = & (k_1 - k_0) d_1 \\ & + \tan^{-1}(\sin(2k_1 d_1) / (\Gamma^{-2} - \cos(2k_1 d_1))) \end{aligned} \quad (4.5)$$

The calibrated formula is independent of the spacing between the antennas. If multiple reflections are neglected, one can obtain a closed form expression for the solution which is given by

$$\Delta \varphi = (k_1 - k_0)d_1 = 2\pi f d_1 (\sqrt{\varepsilon_r} - 1) / c \quad (4.6)$$

by replacing $\Gamma=0$ in (4.5). Although evaluated ε_r in (4.6) cannot achieve a good approximation due to neglect multiple reflections, but, (4.6) can easily be solved for relative dielectric constant as given in (4.7).

$$\varepsilon_r = (1 + c \Delta \varphi / (2\pi f d_1))^2 \quad (4.7)$$

To suppress the effect unwanted reflection absorber material can be used to make a reflection free environment for measurement. **Figure 4.5** shows the implemented setup. Two standard horn antenna used as transmit and receive antenna. Absorber material is placed in different side to avoid undesired reflections from floor and surrounding objects. These reflections can cause error in measured result. Another method to omit unwanted reflections is to use time domain gating which is possible with PNA network used in our measurement. However, only absorber material is used to get rid of reflections. The measurement is done using the setup implemented as in **Figure 4.5**. The phase difference between Silicon slab with 500um and air is shown in **Figure 4.6** and corresponding dielectric constant is depicted in **Figure 4.7**.

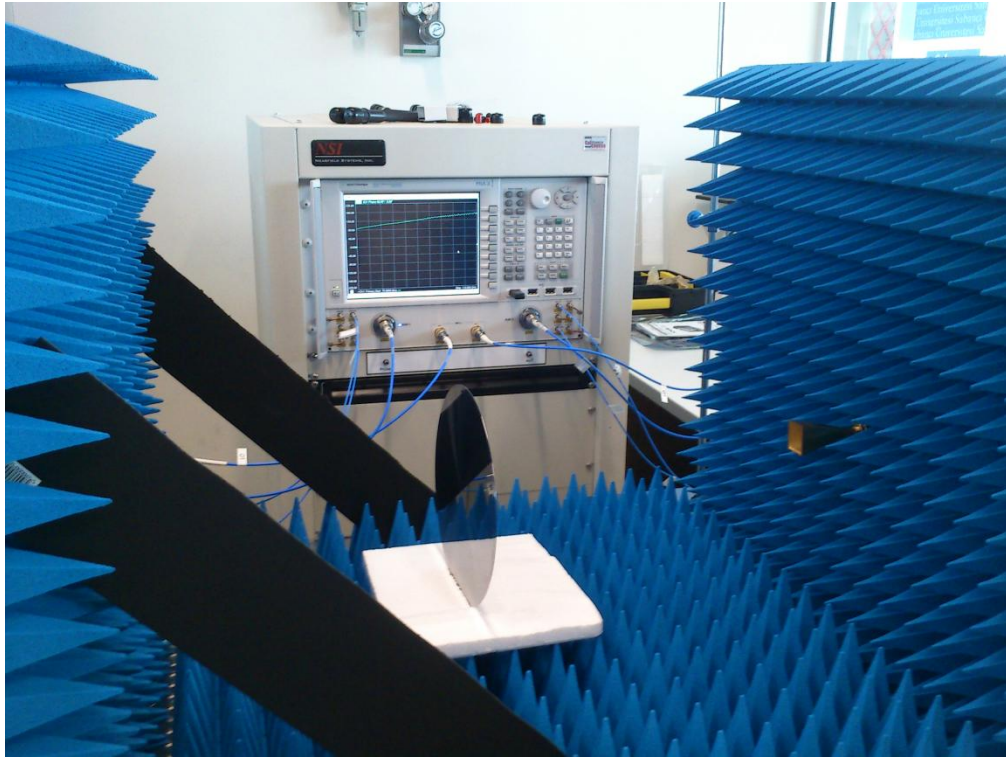


Fig. 4.6 Implemented Dielectric Setup

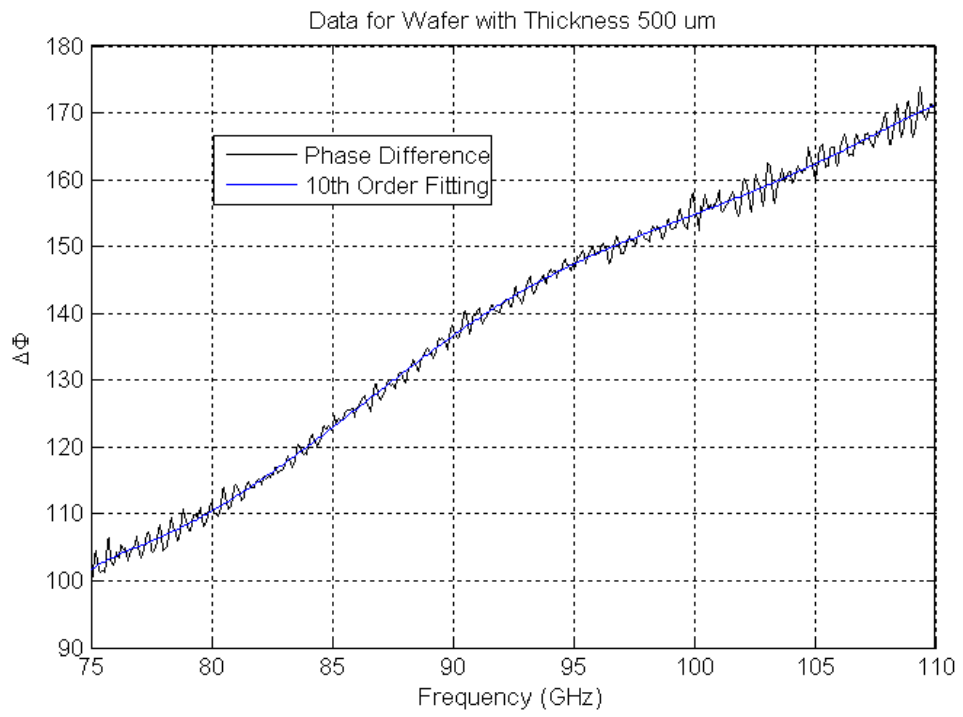


Fig. 4.7 Measured Phase Difference versus Frequency

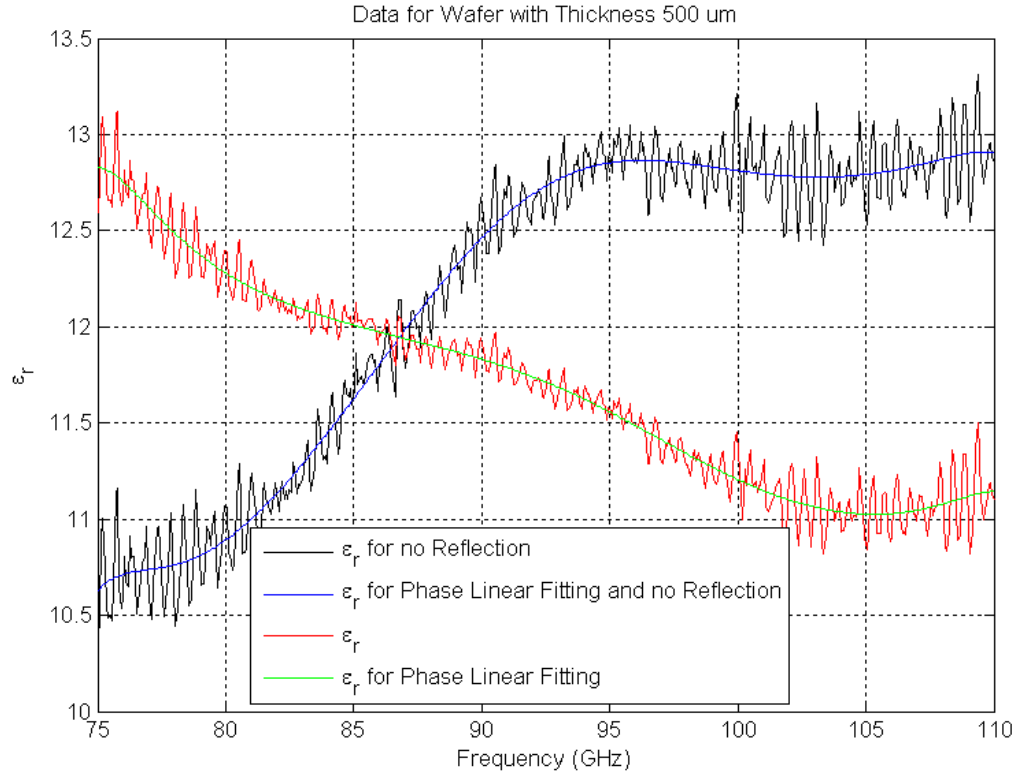


Fig. 4.8 Calculated dielectric constant

Calculated dielectric constant for Silicon can be used for later simulation modeling at full wave simulators. This will allow avoiding frequency shift in response of simulated and measured result.

CONCLUSION AND FUTURE WORK

In this thesis a design of reliable antenna system for automotive radar system at 77GHz is studied. Various type of antenna including dipole antenna and patch type antenna can be used for this purpose. The choice of the antenna is done based on the radar system range (gain requirements), ease of fabrication, possibility of integration with other circuitry and cost. At 77GHz since the size of antenna is small, it is possible to think about on chip antenna design which can integrate the antenna and rest of RF circuitry and make radar compact and cost effective. For this purpose, a design of different antenna like patch, dipole, slot type antenna on Silicon substrate is studied. Patch antenna is selected for final assembly based on the criteria mentioned for 77GHz radar system like gain and fabrication consideration. However, the original antenna on silicon substrate suffers from low gain due to Silicon loss and gain and pattern distortion due to excitation of surface wave. Two approaches is taken to overhaul the problems. First, available etching technique is used to

remove the substrate under the radiating antenna to improve the radiation properties. Second, Electromagnetic band-gap structure is used to filter the unwanted surface wave inside the Silicon substrate. Moreover, further gain improvement is done by array of proposed patch antenna. This also gives the radar system the beam steering option. All the simulations are carried out by FEM based simulator, HFSS. The accuracy of the simulated result is verified with antenna measurement setups implemented at SUNUM laboratory. Antenna setup enables us to conduct S parameter, impedance and radiation pattern measurement. Conducting measurement at this frequency range is a little bit of challenge and requires high tech devices and good practice. A sample of single antenna and antenna in array configuration are realized at IHP Company. Measured results for reflection coefficient of sample dipole antenna from previous works reveal that there is frequency shift between simulated and measured result. This shift can be attributed to the uncertainty about dielectric constant of the Silicon at W-band frequency. In simulation, dielectric constant is assumed to be 12 (low frequency model) for Silicon. However, the difference between simulated and measured result reveals stringent need for knowledge about exact value of Silicon dielectric constant at W-band. So, another chapter is devoted to study the methods of determining the exact value of the Silicon dielectric constant at W band frequency range. Among various techniques, free space method is chosen with two standard horn antennas as transmitter and receiver. Proposed free space method is based on phase information of transmitted signal for different case; the silicon slab between and air. From the phase difference between these two measurements, the dielectric constant of silicon is derived. Advantage of free space is its wideband operation and simple implementation. A dielectric measurement setup is prepared to do the experiment. Measured result seems to properly model for silicon. This result is used to accurately model Silicon substrate for next simulations.

Throughout this thesis, we tried to design reliable antenna system for 77GHz radar system and the focus was on designing on chip antenna. However, antenna design on substrate like Silicon has its own drawbacks. Proposed solutions can mitigate the problems not completely but to some extent. Moreover, the cost of realizing overall chip at foundry is

high for moderate size chip and the price keeps increasing exponentially with the size of chip. Future research study can be focus on designing on chip antenna by replacing the silicon with another low loss, low dielectric constant substrate like FR4. This is possible by using wire-bonding techniques to still keep the single chip solution valid for proposed circuitry. For example, the active circuitry can be realized by foundry process and antenna can be fabricated with low cost printed board technologies. For final assembly, antenna and active part can be connected by wire-bonding techniques.

Reference

- [1] "ECC decision of 19 March 2004 on the frequency band 77–81 GHz to be designated for the use of automotive short range radars," Eur. Radiocommun. Office, Copenhagen, Denmark, (ECC/DEC/(04)03), 2004.[Online]. Available: <http://www.ero.dk>.
- [2] Ali Niknejad and Hossein Hashemi, "*mm-Wave Silicon Technology 60 GHz and beyond*," Springer, 2010.
- [3] Mehdi Seyyed-Esfahlan, Mehmet Kaynak, and Ibrahim Tekin, "77 GHz On-Chip Dipole Type Antennas for Automotive Radar Applications," IEE AWPL, 2014.
- [4] Y. Qian, R.Coccioli, D.Sievenpiper, V.Radisic, E.Yablonovitch, and T.Itoh, "A microstrip patch antenna using novel photonic band-gap structures," *Microwave Journal*, vol. 42, no. 1, pp. 66-76, 1999.
- [5] R.Coccioli, F.R. Yang, K.P. Ma, and T. Itoh, "Aperture-Coupled Patch Antenna on UC-EBG Substrate," *IEEE Trans. Microwave Theory and Techniques*, Vol. 47, pp. 2123 - 2130, 1999.
- [6] R.Garg, P.Bhartia, I.Bahl, and A.Ittipiboon, "*Microstrip Antenna Design Handbook*," Artech House, chapter1, pp 47-55, 2001.
- [7] Ghodgaonkar, D. K., V. V. Varadan, and V. K. Varadan, "A Free-Space Method for Measurement of Dielectric Constants and Loss Tangents at Microwave Frequencies," *IEEE Trans. Inst. and Measurement*, vol. 38, no. 3, pp. 789-793, Jun. 1989.
- [8] G. L. Friedsam and E. M. Biebl, "A Broadband Free-Space Dielectric Properties Measurement System at Millimeter Wavelengths," 1996 Conference on Precision Electromagnetic Measurements Digest, pp. 210–211, Jun. 1996.

- [9] Ghodgaonkar, D. K., V. V. Varadan, and V. K. Varadan, "Free-Space Measurement of Complex Permittivity and Complex Permeability of Magnetic Materials at Microwave Frequencies," *IEEE Trans. Inst. and Measurement*, vol. 39, no. 2, 387-394, Apr. 1990.
- [10] Warren L. Stutzman and Gary A. Thiele, "*Antenna Theory and Design*," Wiley & Sons Pub., 1997.
- [11] D. Sievenpiper, L. Zhang, R. F. Jimenez Broas, N. G. Alexopoulos, and E. Yablonovitch, "High-Impedance Electromagnetic Surfaces with a Forbidden Frequency Band," *IEEE Trans on Microwave and theory and techniques*, Vol. 47, No. 11, 1999.
- [12] R. F. Harrington, "*Time-Harmonic Electromagnetic Field*," Wiley-IEEE Press, 2001.
- [13] V. G. Veselago, "The electrodynamics of substances with simultaneously negative values of ϵ and μ ," *Sov. Phys. Usp.*, Vol. 10, No. 4, 509-514, 1968.
- [14] N. Engheta, R. W. Ziolkowski, "*METAMATERIALS Physics and Engineering Explorations*," 2009.
- [15] C. M. Soukoulis, "Photonic Crystals and Light Localization in the 21st Century," NATO ASI, Series C, Vol. 563, 2001.
- [16] D. R. Smith, W. J. Padilla, D. C. Vier, S. C. Nemat-Nasser, and S. Schultz, "Composite Medium with Simultaneously Negative Permeability and Permittivity," Department of Physics, University of California, San Diego, 1999.
- [17] X. Han, H. Hafdallah Ouslimani, T. Zhang, and A. C. Priou, "CSRRS FOR EFFICIENT REDUCTION OF THE ELECTROMAGNETIC INTERFERENCES AND MUTUAL COUPLING IN MICROSTRIP CIRCUITS," *Progress In Electromagnetic Research B*, Vol. 42, 2012.

[18] L. Brillouin, "*Wave Propagation in Periodic Structures*," 2nd edn., Dover Publications, 2003.

[19] F. Yang, Y. Rahmat-Samii, "Electromagnetic Band Gap Structures in Antenna Engineering," Cambridge University press, 2009.

[20] S. Blanch, J. Romeu and I. Corbella, "Exact representation of Antenna System Diversity Performance from Input Parameter Description," *Electronics Letters*, vol. 39, no. 9, pp. 705–707, 2003.